

12

Carderock Division
David Taylor Research Center

Bethesda, Maryland 20884-5000

AD-A264 835



CDNSWC-SIG-93/108 745 April 1993

Signatures Directorate

Research and Development Report

Evaluation of the Scattered Pressure Due to Infinite Rigid Cylinders, Infinite Elastic Cylindrical Shells, and Rigid Spheres in the Presence of an Ambient Noise Field

by
Rebecca L. Honeycutt
Steven J. Johnson

DTIC
ELECTE
MAY 14 1993
S B D

93 5 13 02 Z

93-10780



64/17



Approved for public release; Distribution is unlimited

CDNSWC-SIG-93/108 745 Evaluation of the Scattered Pressure Due to Infinite Rigid Cylinders, Infinite Elastic Cylindrical Shells, and Rigid Spheres in the Presence of an Ambient Noise Field

MAJOR DTRC TECHNICAL COMPONENTS

CODE 011 DIRECTOR OF TECHNOLOGY, PLANS AND ASSESSMENT

12 SHIP SYSTEMS INTEGRATION DEPARTMENT

14 SHIP ELECTROMAGNETIC SIGNATURES DEPARTMENT

15 SHIP HYDROMECHANICS DEPARTMENT

16 AVIATION DEPARTMENT

17 SHIP STRUCTURES AND PROTECTION DEPARTMENT

18 COMPUTATION, MATHEMATICS & LOGISTICS DEPARTMENT

19 SHIP ACOUSTICS DEPARTMENT

27 PROPULSION AND AUXILIARY SYSTEMS DEPARTMENT

28 SHIP MATERIALS ENGINEERING DEPARTMENT

DTRC ISSUES THREE TYPES OF REPORTS:

1. **DTRC reports, a formal series**, contain information of permanent technical value. They carry a consecutive numerical identification regardless of their classification or the originating department.
2. **Departmental reports, a semiformal series**, contain information of a preliminary, temporary, or proprietary nature or of limited interest or significance. They carry a departmental alphanumeric identification.
3. **Technical memoranda, an informal series**, contain technical documentation of limited use and interest. They are primarily working papers intended for internal use. They carry an identifying number which indicates their type and the numerical code of the originating department. Any distribution outside DTRC must be approved by the head of the originating department on a case-by-case basis.

**Carderock Division
David Taylor Research Center**

Bethesda, Maryland 20084-5000

CDNSWC-SIG-93/108 745

April 1993

**Evaluation of the Scattered Pressure Due
to Infinite Rigid Cylinders, Infinite Elastic
Cylindrical Shells, and Rigid Spheres in the
Presence of an Ambient Noise Field**

by
Rebecca L. Honeycutt
Steven J. Johnson

Approved for public release; Distribution is unlimited

UNCLASSIFIED

SECURITY CLASSIFICATION OF THIS PAGE

REPORT DOCUMENTATION PAGE

1a REPORT SECURITY CLASSIFICATION UNCLASSIFIED			1b RESTRICTIVE MARKINGS none	
2a SECURITY CLASSIFICATION AUTHORITY n/a			3 DISTRIBUTION/AVAILABILITY OF REPORT Approved for Public Release; Distribution is unlimited	
2b DECLASSIFICATION/DOWNGRADING SCHEDULE n/a				
4 PERFORMING ORGANIZATION REPORT NUMBER(S) CDNSWC-SIG-93/108 745			5 MONITORING ORGANIZATION REPORT NUMBER(S)	
6a NAME OF PERFORMING ORGANIZATION Carderock Division, Naval Surface Warfare Center		6b OFFICE SYMBOL (If applicable) Code 745	7a. NAME OF MONITORING ORGANIZATION	
6c ADDRESS (City, State, and ZIP Code) Bethesda, MD 20084-5000			7b. ADDRESS (City, State, and ZIP Code)	
8a NAME OF FUNDING/SPONSORING ORGANIZATION ONR/ONT		8b. OFFICE SYMBOL (If applicable) Code 233	9. PROCUREMENT INSTRUMENT IDENTIFICATION NUMBER	
8c ADDRESS (City, State, and ZIP Code) Arlington, VA 22217-5000			10. SOURCE OF FUNDING NUMBERS	
			PROGRAM ELEMENT NO.	PROJECT NO.
11 TITLE (Include Security Classification) Evaluation of the scattered pressure due to infinite rigid cylinders, infinite elastic cylindrical shells, and rigid spheres in the presence of an ambient noise field				
12 PERSONAL AUTHOR(S) Rebecca L. Honeycutt Steven J. Johnson				
13a TYPE OF REPORT Final		13b. TIME COVERED FROM 1/92 TO 9/92		14. DATE OF REPORT (Year, Month, Day) 1993, April
15. PAGE COUNT 62				
16 SUPPLEMENTARY NOTATION				
17 COSATI CODES			18. SUBJECT TERMS (Continue on reverse if necessary and identify by block number) Ambient Noise Acoustic Scattering	
FIELD	GROUP	SUB-GROUP		
19 ABSTRACT (Continue on reverse if necessary and identify by block number) The sound scattering due to an ambient noise field, approximated by a squared cosine function, is considered for infinite rigid and elastic cylinders and rigid spheres. For the cylinders, it is assumed that the acoustic wave front is parallel to the axis of the cylinder (nformally incident). For this assumption, a closed form expression for the scattered sound field-to-incident ambient noise field (signal-to-noise) ratio is obtained not only for the cosine squared directivity, but for any arbitrary directivity which can be expressed in terms of a Fourier series. For the sphere, it is assumed that the noise is circumferentially symmetric which leads to a closed form expression for the signal-to-noise ratio due to a cosine squared directivity.				
20 DISTRIBUTION/AVAILABILITY OF ABSTRACT <input checked="" type="checkbox"/> UNCLASSIFIED/UNLIMITED <input type="checkbox"/> SAME AS RPT <input type="checkbox"/> DTIC USERS			21. ABSTRACT SECURITY CLASSIFICATION UNCLASSIFIED	
22a NAME OF RESPONSIBLE INDIVIDUAL Dr. Rebecca L. Honeycutt			22b TELEPHONE (Include Area Code) (301) 227-2861	22c. OFFICE SYMBOL Code 745

CONTENTS

	Page
ABSTRACT	1
ADMINISTRATIVE INFORMATION	1
INTRODUCTION	1
MATHEMATICAL FORMULATION	2
CYLINDRICAL SCATTERERS	6
INFINITE RIGID CYLINDER	6
INFINITE ELASTIC CYLINDRICAL SHELL	8
GENERAL DIRECTIONAL DIRECTIVITY	9
<u>Isotropic Noise Field</u>	10
<u>Cosine Squared Directivity</u>	11
NUMERICAL SIMULATIONS	12
RIGID SPHERE	18
CIRCUMFERENTIALLY SYMMETRIC DIRECTIVITY	21
<u>Cosine Squared Directivity</u>	22
NUMERICAL SIMULATIONS	24
CONCLUSIONS	24
APPENDIX A	29
APPENDIX B	31
APPENDIX C	33
APPENDIX D	35
APPENDIX E	39
APPENDIX F	45
REFERENCE	57

FIGURES

Page

1. $10 \log[\mathcal{D}(\phi')]$ for the cosine squared directivity function
with α , β , and γ values of 0.33/75.4, 1.0/75.4, and 33.0/75.4 respectively 14
2. $10 \log[\langle |p_s|^2 \rangle / \langle |p_N|^2 \rangle]$ for infinite rigid cylinders and elastic
cylindrical shells evaluated at $ka = 5$ 15
3. $10 \log[\langle |p_s|^2 \rangle / \langle |p_N|^2 \rangle]$ for infinite rigid cylinders and elastic
cylindrical shells evaluated at $ka = 20$ 16
4. $10 \log[\langle |p_s|^2 \rangle / \langle |p_N|^2 \rangle]$ for infinite rigid cylinders and elastic
cylindrical shells evaluated at $ka = 40$ 17
5. $10 \log[\langle |p_s|^2 \rangle / \langle |p_N|^2 \rangle]$ for a rigid sphere evaluated at $ka = 5$ 26
6. $10 \log[\langle |p_s|^2 \rangle / \langle |p_N|^2 \rangle]$ for a rigid sphere evaluated at $ka = 20$ 27
7. $10 \log[\langle |p_s|^2 \rangle / \langle |p_N|^2 \rangle]$ for a rigid sphere evaluated at $ka = 40$ 28

Accession For		<input checked="" type="checkbox"/>	<input type="checkbox"/>	<input type="checkbox"/>
NTIS GRA&I				
DTIC TAB				
Unannounced				
Justification				
By				
Distribution/				
Availability Codes				
Avail and/or				
Special				
Dist				
A-1				

ABSTRACT

The sound scattering due to an ambient noise field, approximated by a squared cosine function, is considered for infinite rigid and elastic cylinders and rigid spheres. For the cylinders, it is assumed that the acoustic wave front is parallel to the axis of the cylinder (normally incident). For this assumption, a closed form expression for the scattered sound field-to-incident ambient noise field (signal-to-noise) ratio is obtained not only for the cosine squared directivity, but for any arbitrary directivity which can be expressed in terms of a Fourier series. For the sphere, it is assumed that the noise is circumferentially symmetric which leads to a closed form expression for the signal-to-noise ratio due to a cosine squared directivity.

ADMINISTRATIVE INFORMATION

This work was carried out under joint funding from the Acoustic Measurement Facility Improvement Program (AMFIP) and the Office of Naval Research (ONR) Exploratory Development Program. The work was carried out at the Carderock Division of the Naval Surface Warfare Center during January 1992 to September 1992.

INTRODUCTION

The ambient noise of the sea¹ is generated by steady noise sources, such as surface winds, wave interactions, and distant ships as they transit shipping lanes, and by transient sources, such as rain and the calls of marine animals. Although steady sources persist for extended periods of time, their variability leads to the randomness of the ambient noise. Intermittent or transient noise sources also contribute to this variability, but cause greater uncertainty in expected noise levels since their occurrences are less predictable. Since the ambient noise is caused by a variety of sources, its characteristics change throughout the frequency spectrum, with different sources becoming dominant contributors. Different characteristics are also observed at different locations. For instance, tidal currents are more pronounced in coastal waters than in the center of the ocean. In addition to frequency and location, the noise characteris-

tics are affected by changes in sound transmission conditions such as those caused by seasonal changes.

Even though there are a wide variety of sources which can create ambient noise, the two primary contributors are surface noises created by winds and distant shipping noise. We consider frequency ranges high enough that contributions due to shipping noises can be ignored since they exist at much lower frequencies. It has been shown that surface noise contributions extend over a wide range of frequencies and on average are circumferentially symmetric and well approximated by a $\cos^2 \theta$ distribution.² Since the contributions from the surface exceed those from the sea bottom, the noise field will be directional.

The ambient noise field may be thought of as a source which, when incident upon targets such as cylinders, will cause a scattered pressure field. There are two primary concerns about this scattered ambient field. If the scattered pressure is distinguishable from the ambient noise source, it may be possible to use the noise field as a means of imaging the targets.³ The other concern is the effect that the ambient noise scattering may have upon the measurement of these canonical scatterers in scientific experiments.

MATHEMATICAL FORMULATION

The mathematical formulation of the problem begins with a few basic assumptions; measurements are made in a small frequency range and the linear principle of superposition can be applied. Keeping these criteria in mind, the pressure, p_N , at position \mathbf{R} due to an ambient noise distribution can be expressed as a superposition of plane waves, $P_i \exp[i\mathbf{k} \cdot \mathbf{R}]$. Each plane wave has its own propagation direction and amplitude P_i , but they share the same wavenumber k . Therefore, $p_N(\mathbf{R})$ can be expressed as

$$p_N(\mathbf{R}) = \int P_A(\Omega') \exp[i\mathbf{k}' \cdot \mathbf{R}] d\Omega', \quad (1)$$

where $P_A(\Omega')$ is the pressure amplitude with angular dependence expressed in the appropriate

coordinate system, \mathbf{k}' is the vector wavenumber in the direction of propagation, and $d\Omega'$ represents a solid angle integration for the coordinate system.

The scattered pressure from a surface excited by an incident plane wave of amplitude P_i may be formally expressed as $P_i G(\mathbf{R}; \Omega')$ where G is the impulse response function or Green's function for the surface. Applying the superposition principle, the scattered pressure, p_s , at \mathbf{R} due to an ambient noise field is cast in the form

$$p_s(\mathbf{R}) = \int P_A(\Omega') G(\mathbf{R}; \Omega') d\Omega'. \quad (2)$$

The effects of the ambient noise can be determined by measuring the signal-to-noise ratio, S/N , defined by

$$S/N = \left| \frac{P(\mathbf{R}) - p_N(\mathbf{R})}{p_N(\mathbf{R})} \right|^2, \quad (3)$$

where

$$P(\mathbf{R}) = p_N(\mathbf{R}) + p_s(\mathbf{R}) + p_o(\mathbf{R}). \quad (4)$$

is the pressure detected by the hydrophone at \mathbf{R} in the presence of the target, $p_N(\mathbf{R})$ is the pressure detected by the hydrophone in the absence of the target, $p_s(\mathbf{R})$ is the scattered ambient pressure due to the target, and $p_o(\mathbf{R})$ is any other observable pressure. The measured signal-to-noise ratio is then

$$S/N = \left| \frac{p_s(\mathbf{R}) + p_o(\mathbf{R})}{p_N(\mathbf{R})} \right|^2. \quad (5)$$

If the contribution of the scattered noise is large enough, the ambient field can be used for passive imaging. Far from the scattering surface (i.e. $kR \gg 1$), the scattered pressure will diminish significantly as a result of geometrical spreading, and the other observable pressures can be

well estimated by using Eq. 5. Yet if measurements are made close to the scatterer, the scattered noise and other observable noise may not be distinguishable so that the measurements may not be statistically significant.

Since the signal-to-noise ratio is a quantity of interest, we square the expressions for $p_N(\mathbf{R})$ and $p_s(\mathbf{R})$ to obtain

$$|p_N(\mathbf{R})|^2 = \iint P_A(\Omega') P_A^*(\Omega'') \exp[i\mathbf{k}' \cdot \mathbf{R}] \exp[-i\mathbf{k}'' \cdot \mathbf{R}] d\Omega' d\Omega'', \quad (6)$$

and

$$|p_s(\mathbf{R})|^2 = \iint P_A(\Omega') P_A^*(\Omega'') G(\mathbf{R}; \Omega') G^*(\mathbf{R}; \Omega'') d\Omega' d\Omega''. \quad (7)$$

Due to the randomness of the noise field, the mean square pressures, $\langle |p_N(\mathbf{R})|^2 \rangle$ and $\langle |p_s(\mathbf{R})|^2 \rangle$, hold more physical meaning than a single measurement of $p_N(\mathbf{R})$ and $p_s(\mathbf{R})$. Applying this averaging results in

$$\langle |p_N(\mathbf{R})|^2 \rangle = \iint \langle P_A(\Omega') P_A^*(\Omega'') \rangle \exp[i\mathbf{k}' \cdot \mathbf{R}] \exp[-i\mathbf{k}'' \cdot \mathbf{R}] d\Omega' d\Omega'', \quad (8)$$

and

$$\langle |p_s(\mathbf{R})|^2 \rangle = \iint \langle P_A(\Omega') P_A^*(\Omega'') \rangle G(\mathbf{R}; \Omega') G^*(\mathbf{R}; \Omega'') d\Omega' d\Omega''. \quad (9)$$

The term $\langle P_A(\Omega') P_A^*(\Omega'') \rangle$ can be expressed as a directivity function $\mathcal{D}(\Omega', \Omega'')$ by

$$\langle P_A(\Omega') P_A^*(\Omega'') \rangle = |P_I|^2 \mathcal{D}(\Omega', \Omega''), \quad (10)$$

where P_r is a normalization factor. Applying this to Eqs. 8 and 9 results in the signal-to-noise ratio

$$(S/N)_s = \frac{\iint \mathcal{D}(\Omega', \Omega'') G(\mathbf{R}; \Omega') G^*(\mathbf{R}; \Omega'') d\Omega' d\Omega''}{\iint \mathcal{D}(\Omega', \Omega'') \exp[i\mathbf{k}' \cdot \mathbf{R}] \exp[-i\mathbf{k}'' \cdot \mathbf{R}] d\Omega' d\Omega''}. \quad (11)$$

There are two simple directivity functions which do not represent true ambient noise fields, yet are still instructive. The first of these is

$$\mathcal{D}_p(\Omega', \Omega'') = \delta(\Omega' - \Omega_i) \delta(\Omega'' - \Omega_i), \quad (12)$$

which is the directivity for one incident plane wave propagating in the Ω_i direction. The second is

$$\mathcal{D}_{iso}(\Omega', \Omega'') = \mathcal{D}, \quad (13)$$

which indicates no preferred direction and represents an isotropic noise field. A more practical assumption used throughout this paper is that the noise field contains no correlation between angles. This is equivalent to saying

$$\mathcal{D}(\Omega', \Omega'') = \mathcal{D}(\Omega') \delta(\Omega' - \Omega''), \quad (14)$$

which simplifies the signal-to-noise ratio to

$$(S/N)_s = \frac{\int \mathcal{D}(\Omega') G(\mathbf{R}; \Omega') G^*(\mathbf{R}; \Omega') d\Omega'}{\int \mathcal{D}(\Omega') d\Omega'}. \quad (15)$$

CYLINDRICAL SCATTERERS

INFINITE RIGID CYLINDER

In cylindrical coordinates, a wave traveling perpendicularly to the z axis in the direction ϕ' with amplitude P_i can be represented by^{4,5}

$$\begin{aligned} p_{inc}(R, \phi, \phi') &= P_i \exp[ikR \cos(\phi' - \phi)] \\ &= P_i \sum_{n=-\infty}^{\infty} i^n J_n(kR) e^{in(\phi' - \phi)}, \end{aligned} \quad (16)$$

where (R, ϕ) is the location of the receiver, k is the wavenumber, and J_n is the n^{th} order cylindrical Bessel function. When an infinite rigid cylinder of radius a is excited by a normally incident plane wave, the scattered pressure is given by⁴

$$p_s(R, \phi, \phi') = -P_i \sum_{n=-\infty}^{\infty} i^n \frac{J'_n(ka)}{H'_n(ka)} H_n(kR) e^{in(\phi' - \phi)}, \quad (17)$$

where H_n is the cylindrical Hankel function of n^{th} order and the primes on the Bessel and Hankel functions represent differentiation with respect to the arguments of these functions.

When more than one normally incident plane wave excites this cylinder, the principle of superposition can be exploited. With this in mind, the normally incident field representing a spatially continuous noise field of amplitude $P_A(\phi')$ is represented by

$$p_N(\phi) = \int P_A(\phi') \exp[ikR \cos(\phi' - \phi)] d\Omega'. \quad (18)$$

The average incident pressure squared, $\langle |P_N(\phi)|^2 \rangle$, due to this continuous noise source is then

$$\begin{aligned} \langle |p_N(\phi)|^2 \rangle &= \int_{-\pi/2}^{3\pi/2} d\phi' \int_{-\pi/2}^{3\pi/2} d\phi'' \langle P_A(\phi') P_A^*(\phi'') \rangle \\ &\quad \cdot \exp[ikR \cos(\phi' - \phi)] \exp[-ikR \cos(\phi'' - \phi)]. \end{aligned} \quad (19)$$

In the same manner, the scattered pressure due to this continuous noise source is represented by

$$p_s(\phi) = - \int P_A(\phi') \sum_{n=-\infty}^{\infty} i^n \frac{J'_n(ka)}{H'_n(ka)} H_n(kR) e^{in(\phi' - \phi)} d\Omega', \quad (20)$$

The average scattered pressure squared, $\langle |p_s(\phi)|^2 \rangle$, is subsequently represented by

$$\begin{aligned} \langle |p_s(\phi)|^2 \rangle &= \int_{-\pi/2}^{3\pi/2} d\phi' \int_{-\pi/2}^{3\pi/2} d\phi'' \langle P_A(\phi') P_A^*(\phi'') \rangle \\ &\quad \cdot \sum_{n=-\infty}^{\infty} \left[i^n \frac{J'_n(ka)}{H'_n(ka)} H_n(kR) e^{in(\phi' - \phi)} \right] \\ &\quad \cdot \sum_{r=-\infty}^{\infty} \left[i^r \frac{J'_r(ka)}{H'_r(ka)} H_r(kR) e^{ir(\phi'' - \phi)} \right]^* . \end{aligned} \quad (21)$$

Define T_n^R by

$$T_n^R = i^n \frac{J'_n(ka)}{H'_n(ka)} H_n(kR) \quad (22)$$

and define $\mathcal{D}(\phi', \phi'')$, the directivity function associated with the noise field, by

$$\langle P_A(\phi') P_A^*(\phi'') \rangle = \mathcal{D}(\phi', \phi'') |P_I|^2 . \quad (23)$$

Using these definitions, Eqs. 19 and 21 simplify to

$$\frac{\langle |p_s(\phi)|^2 \rangle}{|P_I|^2} = \int_{-\pi/2}^{3\pi/2} d\phi' \int_{-\pi/2}^{3\pi/2} d\phi'' \mathcal{D}(\phi', \phi'') \exp[ikR(\cos(\phi' - \phi) - \cos(\phi'' - \phi))] \quad (24)$$

and

$$\frac{\langle |p_s(\phi)|^2 \rangle}{|P_I|^2} = \int_{-\pi/2}^{3\pi/2} d\phi' \int_{-\pi/2}^{3\pi/2} d\phi'' \mathcal{D}(\phi', \phi'') \sum_{n=-\infty}^{\infty} \sum_{r=-\infty}^{\infty} T_n^R T_r^{R*} e^{in(\phi' - \phi)} e^{-ir(\phi'' - \phi)} \quad (25)$$

respectively. The next assumption made is that the noise field is spatially uncorrelated so that

$$\mathcal{D}(\phi', \phi'') = \mathcal{D}(\phi') \delta(\phi' - \phi''). \quad (26)$$

Applying this to Eq. 24 yields

$$\begin{aligned} \frac{\langle |p_N(\phi)|^2 \rangle}{|P_I|^2} &= \int_{-\pi/2}^{3\pi/2} d\phi' \mathcal{D}(\phi') \exp[ikR \cos(\phi' - \phi)] \exp[-ikR \cos(\phi' - \phi)] \\ &= \int_{-\pi/2}^{3\pi/2} d\phi' \mathcal{D}(\phi'). \end{aligned} \quad (27)$$

Applying Eq. 26 to Eq. 25 and interchanging the order of the summations and integrations results in

$$\frac{\langle |p_s(\phi)|^2 \rangle}{|P_I|^2} = \sum_{n=-\infty}^{\infty} \sum_{r=-\infty}^{\infty} T_n^R T_r^{R*} e^{-i(n-r)\phi} \int_{-\pi/2}^{3\pi/2} \mathcal{D}(\phi') e^{i(n-r)\phi'} d\phi'. \quad (28)$$

INFINITE ELASTIC CYLINDRICAL SHELL

The scattered pressure from an infinite elastic cylindrical shell excited by an incident plane wave propagating in the direction ϕ' is given by⁴

$$p_{se}(\phi, \phi') = -P_{inc} \sum_{n=-\infty}^{\infty} i^n \frac{H_n(kR)}{H'_n(ka)} \left[J'_n(ka) - \frac{2\rho c}{(Z_n + z_n)\pi ka H'_n(ka)} \right] e^{in(\phi' - \phi)}. \quad (29)$$

The modal structural impedance Z_n is defined by

$$Z_n = -\frac{i\rho_s c_p}{\Omega} \cdot \frac{h}{a} \cdot \frac{\Omega^4 - \Omega^2(1 + n^2 + \beta^2 n^4) + \beta^2 n^6}{\Omega^2 - n^2}, \quad (30)$$

where h/a is the thickness to radius ratio, $\beta^2 = (h/a)^2/12$ is a nondimensional thickness parameter, $\Omega = \omega a/c_p$ is a nondimensional frequency parameter, c_p is the compressional wave speed, and ρ_s is the density of the structure. The specific acoustic impedance z_n is defined by

$$z_n = i\rho c \frac{H_n(ka)}{H'_n(ka)}, \quad (31)$$

where ρ is the fluid density.

By defining T_n^E to be

$$T_n^E = i^n \frac{H_n(kR)}{H'_n(ka)} \left[J'_n(ka) - \frac{2\rho c}{(Z_n + z_n)\pi ka H'_n(ka)} \right], \quad (32)$$

Equations 27 and 28 of the rigid cylinder case may be used for an elastic cylindrical shell by substituting T_n^E for T_n^R . In the formulations to follow, T_n will be used to represent T_n^R and T_n^E , resulting in generalized equations.

GENERAL DIRECTIONAL DIRECTIVITY

We will assume that the noise is normally incident on the cylinder so that the directivity function in cylindrical coordinates is dependent only on the angle ϕ . Although this is not the most realistic case, it is a solvable problem and serves as a first estimate. A general directional directivity function of this sort, $\mathcal{D}(\phi')$, can be expressed in terms of its Fourier series expansion as

$$\mathcal{D}(\phi') = \begin{cases} \sum_{m=-\infty}^{\infty} a_m e^{im\phi'}, & -\pi/2 \leq \phi' \leq \pi/2 \\ \sum_{m=-\infty}^{\infty} b_m e^{im\phi'}, & \pi/2 \leq \phi' \leq 3\pi/2, \end{cases} \quad (33)$$

where a_m and b_m are the Fourier series coefficients which are determined for the ambient field of interest. For this directivity function, the average noise strength becomes

$$\frac{\langle |p_N|^2 \rangle}{|P_I|^2} = \sum_{m=-\infty}^{\infty} a_m \int_{-\pi/2}^{\pi/2} e^{im\phi'} d\phi' + \sum_{m=-\infty}^{\infty} b_m \int_{\pi/2}^{3\pi/2} e^{im\phi'} d\phi', \quad (34)$$

and the average scattered field yields

$$\begin{aligned} \frac{\langle |p_s|^2 \rangle}{|P_I|^2} = \sum_{n=-\infty}^{\infty} \sum_{r=-\infty}^{\infty} T_n T_r^* e^{-i(n-r)\phi} & \left[\sum_{m=-\infty}^{\infty} a_m \int_{-\pi/2}^{\pi/2} e^{i(n-r+m)\phi'} d\phi' \right. \\ & \left. + \sum_{m=-\infty}^{\infty} b_m \int_{\pi/2}^{3\pi/2} e^{i(n-r+m)\phi'} d\phi' \right]. \end{aligned} \quad (35)$$

In Eq. 35, T_n represents either T_n^R or T_n^E , depending upon the case of interest.

Upon the simplifications of Appendix B, these expressions become

$$\frac{\langle |p_N|^2 \rangle}{|P_I|^2} = \pi(a_0 + b_0) + 2 \sum_{m=-\infty}^{\infty} (a_m - b_m) \frac{(-1)^{(m-1)/2}}{m} \delta_{m,odd} \quad (36)$$

and

$$\begin{aligned} \frac{\langle |p_s|^2 \rangle}{|P_I|^2} = \pi \sum_{m=-\infty}^{\infty} (a_m + b_m) e^{im\phi} \sum_{n=-\infty}^{\infty} T_n T_{n+m}^* \\ + 2 \sum_{m=-\infty}^{\infty} (a_m - b_m) \sum_{n=-\infty}^{\infty} \sum_{r=-\infty}^{\infty} T_n T_r^* \\ \cdot \frac{e^{-i(n-r)\phi} (-1)^{(n-r+m-1)/2}}{(n-r+m)} \delta_{n-r+m,odd}. \end{aligned} \quad (37)$$

Isotropic Noise Field

An isotropic noise field is one in which the noise is evenly distributed in all directions. The directivity, $\mathcal{D}_{iso}(\phi')$, is therefore a constant so that the Fourier series coefficients are $a_0 = b_0$

and $a_m = b_m = 0 \quad \forall m \geq 1$. The resulting isotropic noise field is given by

$$\frac{\langle |p_N|^2 \rangle_{iso}}{|P_I|^2} = 2\pi a_0 \quad (38)$$

and the isotropic scattered field is given by

$$\frac{\langle |p_S|^2 \rangle_{iso}}{|P_I|^2} = 2\pi a_0 \sum_{n=-\infty}^{\infty} T_n T_n^*. \quad (39)$$

Since the incident field is independent of angle, the scattered pressure is also angularly independent which is seen in Eq. 39. The signal-to-noise ratio resulting from an isotropic field is subsequently

$$\frac{\langle |p_S|^2 \rangle_{iso}}{\langle |p_N|^2 \rangle_{iso}} = \sum_{n=-\infty}^{\infty} T_n T_n^*. \quad (40)$$

Cosine Squared Directivity

An example of a physically significant directivity is one which can be represented as a directional $\cos^2 \phi$ function.² The directivity function in cylindrical coordinates is thus prescribed by

$$\mathcal{D}(\phi') = \begin{cases} \alpha + \beta \cos^2 \phi', & -\pi/2 \leq \phi' \leq \pi/2 \\ \alpha + \gamma \cos^2 \phi', & \pi/2 \leq \phi' \leq 3\pi/2. \end{cases} \quad (41)$$

The Fourier coefficients for this specific field are $a_0 = \alpha + \beta/2$, $a_{-2} = a_2 = \beta/4$, $b_0 = \alpha + \gamma/2$, and $b_{-2} = b_2 = \gamma/4$. Applying these coefficients to Eq. 36 yields

$$\frac{\langle |p_N|^2 \rangle}{|P_I|^2} = \pi[2\alpha + (\beta + \gamma)/2]. \quad (42)$$

Applying the same coefficients to Eq. 37 yields

$$\begin{aligned}
\frac{\langle |p_s|^2 \rangle}{|P_I|^2} = & \pi[2\alpha + (\beta + \gamma)/2] \sum_{n=-\infty}^{\infty} T_n T_n^* \\
& + \pi(\beta + \gamma)/4 \sum_{n=-\infty}^{\infty} [e^{2i\phi} T_n T_{n+2}^* + e^{-2i\phi} T_n T_{n-2}^*] \\
& - (\beta - \gamma)/2 \sum_{n=-\infty}^{\infty} \sum_{r=-\infty}^{\infty} T_n T_r^* e^{-i(n-r)\phi} (-1)^{(n-r-1)/2} \\
& \cdot \left[\frac{1}{(n-r-2)} - \frac{2}{n-r} + \frac{1}{(n-r+2)} \right] \delta_{n-r, \text{odd}},
\end{aligned} \tag{43}$$

resulting in a signal-to-noise ratio of

$$\begin{aligned}
\frac{\langle |p_s|^2 \rangle}{\langle |p_N|^2 \rangle} = & \sum_{n=-\infty}^{\infty} T_n T_n^* + \frac{\beta + \gamma}{2(4\alpha + \beta + \gamma)} \sum_{n=-\infty}^{\infty} [e^{2i\phi} T_n T_{n+2}^* + e^{-2i\phi} T_n T_{n-2}^*] \\
& - \frac{\beta - \gamma}{\pi(4\alpha + \beta + \gamma)} \sum_{n=-\infty}^{\infty} \sum_{r=-\infty}^{\infty} T_n T_r^* e^{-i(n-r)\phi} (-1)^{(n-r-1)/2} \\
& \cdot \left[\frac{1}{(n-r-2)} - \frac{2}{n-r} + \frac{1}{(n-r+2)} \right] \delta_{n-r, \text{odd}}.
\end{aligned} \tag{44}$$

Note that the first term of the right hand side of this equation is just the signal-to-noise ratio of the isotropic field.

NUMERICAL SIMULATIONS

Measured values of a surface directivity led to α , β , and γ values of 0.33/75.4, 1.0/75.4, and 33.0/75.4 respectively.⁶ Our numerical simulations were carried out using the MATLAB program `cyl_inf_rig_elas` which can be found in Appendix F. These simulations are for ka values of 5, 20, and 40 respectively and kR values of $16ka$ and $32ka$ which represent experimental measurement distances.

Before performing numerical simulations on an elastic cylinder, the impedance term of Eq. 32 is expressed in terms of the non-dimensional variables a/h , c/c_p , and ρ/ρ_s , so that

$$T_n^E = i^n \frac{H_n(kR)}{H'_n(ka)} \left[J'_n(ka) + \frac{2i}{\pi} \frac{c}{c_p} \frac{N_n(\Omega)}{D_n(\Omega)} \right], \quad (45)$$

where

$$N_n(\Omega) = (\Omega^2 - n^2), \quad (46)$$

and

$$D_n(\Omega) = H_n(ka)\Omega(\Omega^2 - n^2) - \frac{\rho_s}{\rho} \frac{c_p}{c} \frac{h}{a} H'_n(ka) \left[\Omega^4 - \Omega^2(1 + n^2 + \beta^2 n^4) + \beta^2 n^6 \right]. \quad (47)$$

For our simulations, the non-dimensional variables were given values of $a/h = 100$, $c_p/c = 3.5$, and $\rho_s/\rho = 7.5$

Since we deal mainly in target strength, we have plotted $10 \log[\langle |p_s|^2 \rangle / \langle |p_N|^2 \rangle]$ with respect to angle for infinite rigid cylinders and infinite elastic cylindrical shells. In Figs. 1, 2, and 3, all solid lines indicate rigid results while all the dashed lines indicate elastic results. For each figure, the outer pair of curves is the function evaluated at $kR = 16 * ka$, while the inner set of curves is an evaluation at $kR = 32 * ka$. For high ka , the decrease in horizontal scattering ($\phi = -\pi/2$ and $\phi = \pi/2$) becomes more pronounced and in both the rigid and elastic cases, the foward scattering from $\phi = 0$ is greater than the backscattering from this direction. In a comparison of the elastic and rigid scattering, the foward scattering is more dominant in the elastic case for small ka . In each figure it is also seen that the difference between the $16 * ka$ case and the $32 * ka$ case is on the order of 3 dB as would be expected when comparing cylindrical scattering at distances which differ by a factor of two.

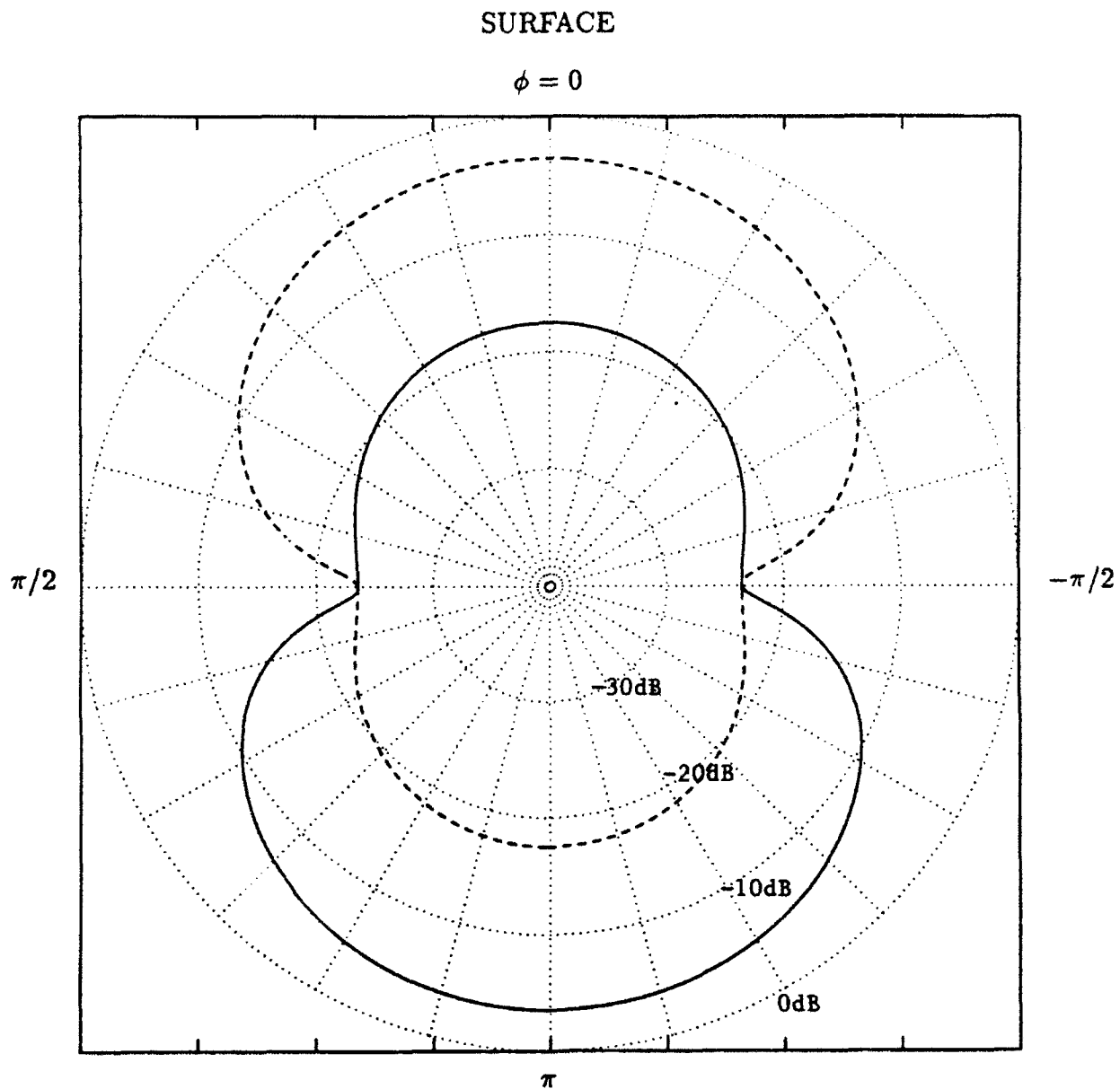


Fig. 1. $10 \log[D(\phi)]$ for the cosine squared directivity function with α , β , and γ values of 0.33/75.4, 1.0/75.4, and 33.0/75.4 respectively. ϕ indicates the direction of propagation (solid) and the direction from which the wave comes (dashed). The center of the plot indicates the axis of the cylinder.

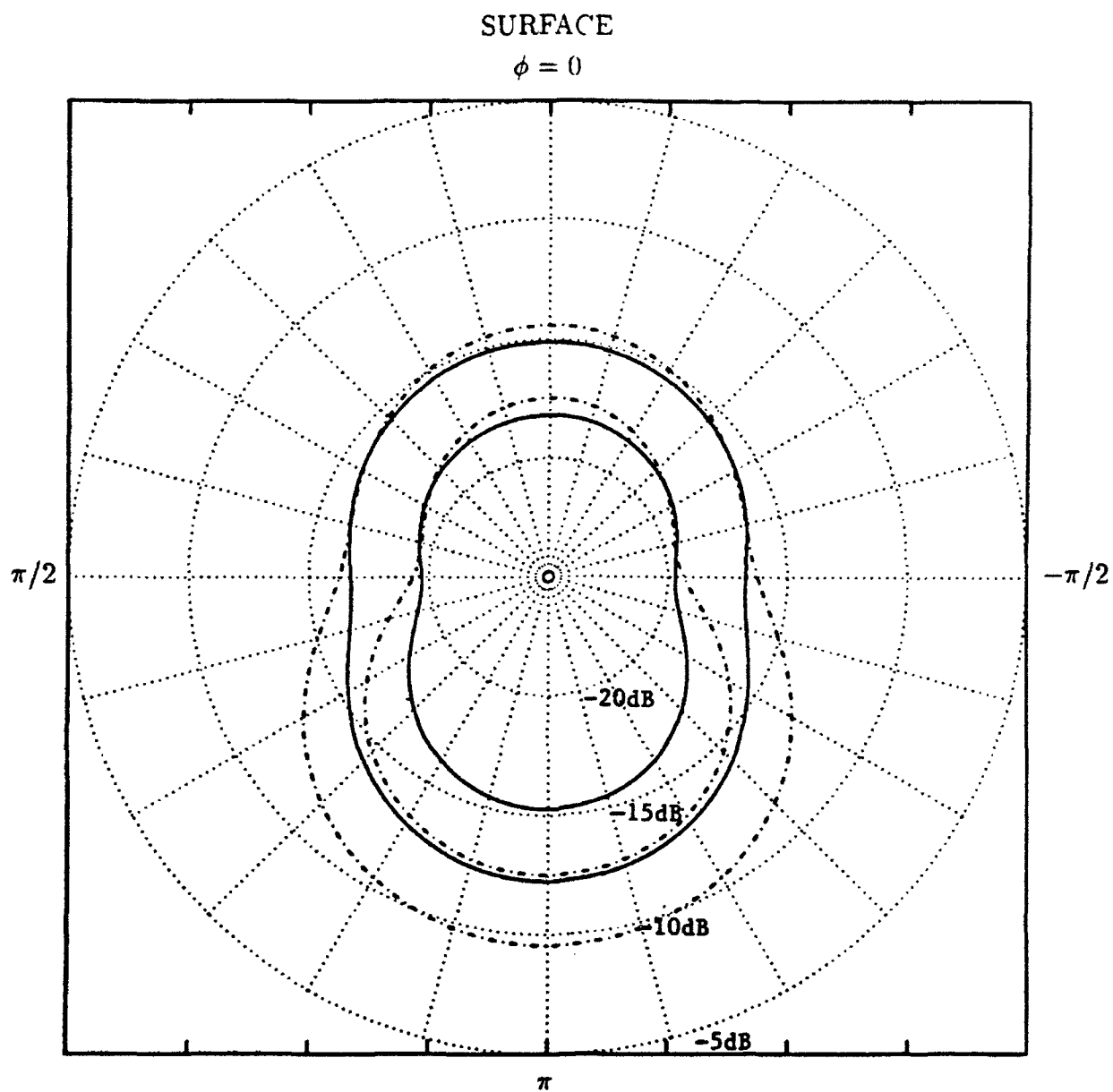


Fig. 2. $10\log[\langle |p_s|^2 \rangle / \langle |p_N|^2 \rangle]$ for infinite rigid cylinders and elastic cylindrical shells evaluated at $ka = 5$. The outer solid(dashed) line corresponds to the rigid(elastic) result for $kR = 16 * ka$. The inner solid(dashed) line corresponds to the rigid(elastic) result for $kR = 32 * ka$. The center of the plot indicates the axis of the cylinder.

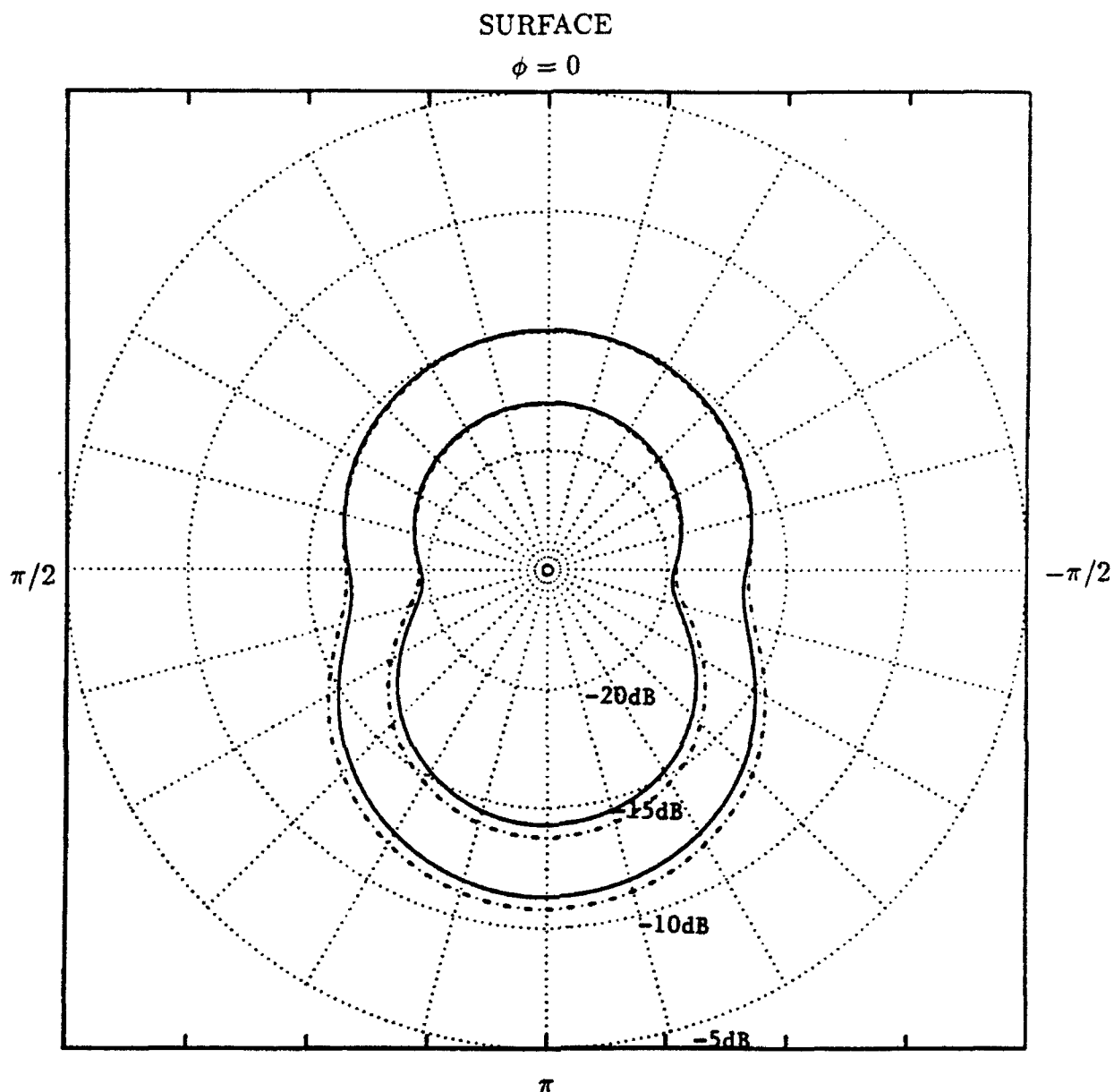


Fig. 3. $10 \log[|p_s|^2/|p_N|^2]$ for infinite rigid cylinders and elastic cylindrical shells evaluated at $ka = 20$. The outer solid(dashed) line corresponds to the rigid(elastic) result for $kR = 16 * ka$. The inner solid(dashed) line corresponds to the rigid(elastic) result for $kR = 32 * ka$. The center of the plot indicates the axis of the cylinder.

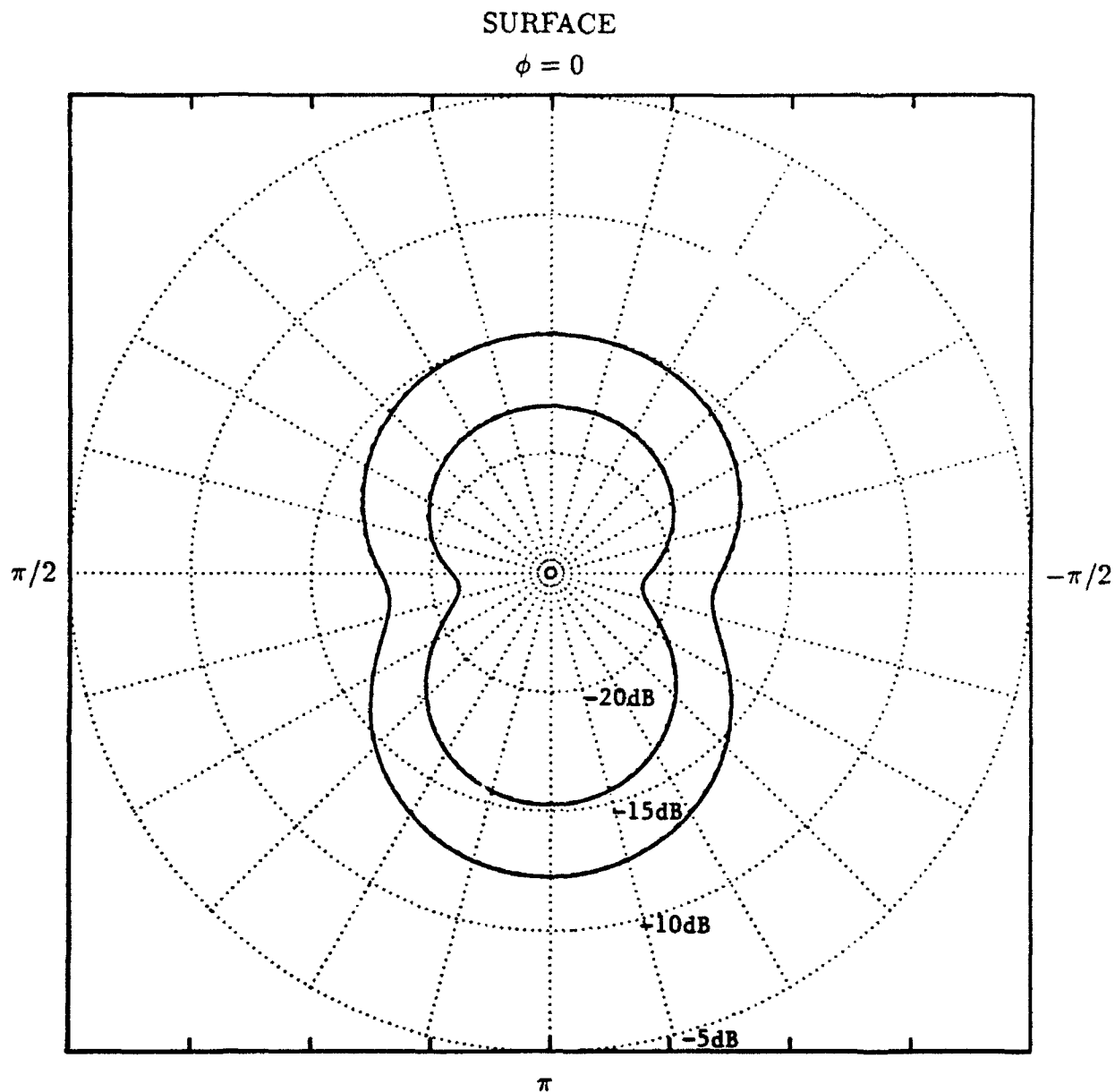


Fig. 4. $10 \log[\langle |p_s|^2 \rangle / \langle |p_N|^2 \rangle]$ for infinite rigid cylinders and elastic cylindrical shells evaluated at $ka = 40$. The outer solid(dashed) line corresponds to the rigid(elastic) result for $kR = 16 * ka$. The inner solid(dashed) line corresponds to the rigid(elastic) result for $kR = 32 * ka$. The center of the plot indicates the axis of the cylinder.

RIGID SPHERE

The incident pressure, p_{inc} , in spherical coordinates for a plane wave propagating in the positive z direction is given by^{4,5}

$$\begin{aligned} p_{inc}(R, \theta) &= P_i \exp[ikR \cos \theta] \\ &= P_i \sum_{n=0}^{\infty} (2n+1) i^n P_n(\cos \theta) j_n(kR), \end{aligned} \quad (48)$$

where P_i is the amplitude of the wave, and (R, θ) indicates the location of the observation point with θ , the azimuthal angle, measured from the positive z axis. P_n is the n^{th} order Legendre polynomial and j_n is the n^{th} order spherical Bessel function. Since the wave is propagating in the z direction, there is no circumferential angular dependence. The scattered pressure, p_s , due to this incident wave striking a rigid sphere of radius a is

$$p_s(R, \theta) = -P_i \sum_{n=0}^{\infty} (2n+1) i^n P_n(\cos \theta) \frac{j'_n(ka)}{h'_n(ka)} h_n(kR), \quad (49)$$

where h_n is the n^{th} order spherical Hankel function, and the primes indicate derivatives with respect to the arguments.

For a general result we consider a plane wave propagating in the (θ', ϕ') direction which is viewed from the (θ, ϕ) direction where ϕ and ϕ' represent circumferential angles. Let ψ indicate the angle between the two directions given above. The relation between ψ and the other angles is

$$\cos \psi = \cos \theta \cos \theta' + \sin \theta \sin \theta' \cos(\phi - \phi'). \quad (50)$$

The angle ψ now replaces the θ of Eqs. 48 and 49 so that the Legendre polynomials become $P_n(\cos \psi)$ rather than $P_n(\cos \theta)$. Applying Eqs. 3 to 5 of Appendix A to $P_n(\cos \psi)$ changes the

general incident and scattered pressures to

$$p_{inc}(R, \theta, \phi, \theta', \phi') = P_i \exp[ikR(\cos \theta \cos \theta' + \sin \theta \sin \theta' \cos(\phi - \phi'))]. \quad (51)$$

and

$$p_s(R, \theta, \phi, \theta', \phi') = -P_i \sum_{n=0}^{\infty} \sum_{m=0}^n \epsilon_m \chi_{n,m} P_n^m(\cos \theta) P_n^m(\cos \theta') \cos[m(\phi - \phi')] \quad (52)$$

respectively. $\chi_{m,n}$ is defined to be to be

$$\chi_{n,m} = (2n+1) \frac{(n-m)!}{(n+m)!} T_n^S, \quad (53)$$

where T_n^S is defined in terms of spherical bessel functions as

$$T_n^S = i^n \frac{j_n'(ka)}{h_n'(ka)} h_n(kR), \quad (54)$$

in the same manner as the rigid cylindrical case. ϵ_m indicates the Neumann function defined in Eq. 77 of Appendix A. From this point we suppress the S superscript.

Equations 51 and 52 are the incident and scattered pressure due to one plane wave. As in the cylindrical formulation, the principle of superposition is used to generalize to the situation of a spatially continuous noise field. The continuous incident and scattered pressure become

$$p_N(\theta, \phi) = \int P_A(\theta', \phi') \exp[ikR(\cos \theta \cos \theta' + \sin \theta \sin \theta' \cos(\phi - \phi'))] d\Omega' \quad (55)$$

and

$$p_s(\theta, \phi) = - \int P_A(\theta', \phi') \sum_{n=0}^{\infty} \sum_{m=0}^n \epsilon_m \chi_{n,m} P_n^m(\cos \theta) P_n^m(\cos \theta') \cos[m(\phi - \phi')] d\Omega', \quad (56)$$

where the solid angle integration $d\Omega'$ is given by $d\Omega' = \sin \theta' d\theta' d\phi'$ and $P_A(\theta', \phi')$ is the directional amplitude for the wave. The average incident pressure squared at any point is indicated by

$$\begin{aligned} \langle |p_N(\theta, \phi)|^2 \rangle &= \int_0^\pi \int_0^{2\pi} \sin \theta' d\theta' d\phi' \int_0^\pi \int_0^{2\pi} \sin \theta'' d\theta'' d\phi'' \langle P_A(\theta', \phi') P_A^*(\theta'', \phi'') \rangle \\ &\quad \cdot \exp[ikR(\cos \theta \cos \theta' + \sin \theta \sin \theta' \cos(\phi - \phi'))] \\ &\quad \cdot \exp[-ikR(\cos \theta \cos \theta'' + \sin \theta \sin \theta'' \cos(\phi - \phi''))]. \end{aligned} \quad (57)$$

Similarly the average scattered pressure squared at any point is indicated by

$$\begin{aligned} \langle |p_s(\theta, \phi)|^2 \rangle &= \int_0^\pi \int_0^{2\pi} \sin \theta' d\theta' d\phi' \int_0^\pi \int_0^{2\pi} \sin \theta'' d\theta'' d\phi'' \langle P_A(\theta', \phi') P_A^*(\theta'', \phi'') \rangle \\ &\quad \cdot \sum_{n=0}^{\infty} \sum_{m=0}^n \epsilon_m \chi_{n,m} P_n^m(\cos \theta) P_n^m(\cos \theta') \cos[m(\phi - \phi')] \\ &\quad \cdot \sum_{j=0}^{\infty} \sum_{k=0}^j \epsilon_k \chi_{j,k}^* P_j^k(\cos \theta) P_j^k(\cos \theta'') \cos[k(\phi - \phi'')]. \end{aligned} \quad (58)$$

Let the correlation between the pressure amplitudes be defined as

$$\langle P_A(\theta', \phi') P_A^*(\theta'', \phi'') \rangle = |P_I|^2 \mathcal{D}(\theta', \phi', \theta'', \phi''), \quad (59)$$

where $\mathcal{D}(\theta', \phi', \theta'', \phi'')$ indicates the directivity function associated with the noise field. As in the cylindrical case we assume that the pressure fields from different directions are uncorrelated so that the directivity function reduces to

$$\mathcal{D}(\theta', \phi', \theta'', \phi'') = \mathcal{D}(\theta', \phi') \delta(\mathbf{x}) = \mathcal{D}(\theta', \phi') \frac{\delta(\theta' - \theta'') \delta(\phi' - \phi'')}{\sin \theta'}. \quad (60)$$

Applying these definitions to Eqs. 57 and 58 yields

$$\begin{aligned}
\frac{\langle |p_N(\theta, \phi)|^2 \rangle}{|P_I|^2} &= \int_0^\pi \int_0^{2\pi} \sin \theta' d\theta' d\phi' \mathcal{D}(\theta', \phi') \\
&\quad \cdot \exp[ikR(\cos \theta \cos \theta' + \sin \theta \sin \theta' \cos(\phi - \phi'))] \\
&\quad \cdot \exp[-ikR(\cos \theta \cos \theta' + \sin \theta \sin \theta' \cos(\phi - \phi'))] \\
&= \int_0^\pi \int_0^{2\pi} \sin \theta' d\theta' d\phi' \mathcal{D}(\theta', \phi'),
\end{aligned} \tag{61}$$

and

$$\frac{\langle |p_s(\theta, \phi)|^2 \rangle}{|P_I|^2} = \sum_{n=0}^{\infty} \sum_{m=0}^n \sum_{j=0}^{\infty} \sum_{k=0}^j \epsilon_m \epsilon_k \chi_{n,m} \chi_{j,k}^* P_n^m(\cos \theta) P_j^k(\cos \theta) I(n, m, j, k), \tag{62}$$

where

$$\begin{aligned}
I(n, m, j, k) &= \int_0^\pi \int_0^{2\pi} d\theta' d\phi' \sin \theta' P_n^m(\cos \theta') P_j^k(\cos \theta') \mathcal{D}(\theta', \phi') \\
&\quad \cdot \cos[m(\phi - \phi')] \cos[k(\phi - \phi')].
\end{aligned} \tag{63}$$

CIRCUMFERENTIALLY SYMMETRIC DIRECTIVITY

In the case that the directivity is circumferentially symmetric, $\mathcal{D}(\theta', \phi') = \mathcal{D}(\theta')$, the resulting average noise field is

$$\frac{\langle |p_N(\theta, \phi)|^2 \rangle}{|P_I|^2} = 2\pi \int_0^\pi \mathcal{D}(\theta') \sin \theta' d\theta'. \tag{64}$$

After the simplifications of Appendix C have been made, the scattered pressure field reduces to

$$\frac{\langle |p_s(R, \theta, \phi)|^2 \rangle}{|P_I|^2} = 2\pi \sum_{n=0}^{\infty} \sum_{j=0}^{\infty} (2n+1)(2j+1) T_n T_j^* \sum_{m=0}^{\min[n,j]} S_{n,j,m}, \tag{65}$$

where

$$S_{n,j,m} = \epsilon_m \frac{(n-m)! (j-m)!}{(n+m)! (j+m)!} P_n^m(\cos \theta) P_j^m(\cos \theta) I_{\theta'}(n, m, j, m) \quad (66)$$

and

$$I_{\theta'}(n, m, j, k) = \int_0^\pi \sin \theta' P_n^m(\cos \theta') P_j^k(\cos \theta') \mathcal{D}(\theta') d\theta'. \quad (67)$$

For every pair (n, j) , there is also a pair (j, n) which gives the same $S_{n,j,m}$. However, $T_n T_j^*$ becomes $T_j T_n^*$. By introducing a change to the summation limits, the expression for the scattered pressure becomes

$$\frac{\langle |p_s|^2 \rangle}{|P_i|^2} = \pi \sum_{n=0}^{\infty} \sum_{j=0}^n (2n+1)(2j+1) [T_n T_j^* + T_j T_n^*] \epsilon_{(n-j)} \sum_{m=0}^j S_{n,j,m}. \quad (68)$$

Cosine Squared Directivity

We define $\mathcal{D}(\theta')$ as we did in the case of the cylinder, but give it circumferential symmetry.

Therefore

$$\mathcal{D}(\theta') = \begin{cases} \alpha + \beta \cos^2 \theta', & 0 \leq \theta' \leq \pi/2 \\ \alpha + \gamma \cos^2 \theta', & \pi/2 \leq \theta' \leq \pi. \end{cases} \quad (69)$$

The average noise field for this directivity becomes

$$\begin{aligned} \frac{\langle |p_N(\theta, \phi)|^2 \rangle}{|P_i|^2} &= 2\pi \left[\alpha \int_0^\pi \sin \theta' d\theta' + \beta \int_0^{\pi/2} \cos^2 \theta' \sin \theta' d\theta' + \gamma \int_{\pi/2}^\pi \cos^2 \theta' \sin \theta' d\theta' \right] \\ &= 2\pi [2\alpha + (\beta + \gamma)/3]. \end{aligned} \quad (70)$$

After the simplifications of Appendix E have been made, the average scattered pressure becomes

$$\begin{aligned}
\frac{\langle |p_s|^2 \rangle}{|P_I|^2} = & 4\pi\alpha \sum_{n=0}^{\infty} (2n+1) T_n T_n^* \\
& + 2\pi(\beta + \gamma) \cdot \left\{ \begin{aligned} & \sum_{n=0}^{\infty} [T_n T_n^*] \sum_{m=0}^n \epsilon_m P_n^{-m}(\cos \theta) P_n^{-m}(\cos \theta) \frac{(n-m+1)(n+m+1)!}{(2n+3)(n-m)!} \\ & + \sum_{n=2}^{\infty} [T_n T_{n-2}^* + T_{n-2} T_n^*] \\ & \quad \cdot \sum_{m=0}^{n-2} \epsilon_m P_n^{-m}(\cos \theta) P_{n-2}^{-m}(\cos \theta) \frac{1}{(2n-1)} \frac{(n+m)!}{(n-m-2)!} \\ & + \sum_{n=1}^{\infty} [T_n T_n^*] \sum_{m=0}^{n-1} \epsilon_m P_n^{-m}(\cos \theta) P_n^{-m}(\cos \theta) \frac{(n+m)}{(2n-1)} \frac{(n+m)!}{(n-m-1)!} \end{aligned} \right\} \\
& + 2\pi(\beta - \gamma) \cdot \left\{ \begin{aligned} & \sum_{n=1}^{\infty} \sum_{j=0}^{n-1} \delta_{n+j, \text{odd}} [T_n T_j^* + T_j T_n^*] \sum_{m=0}^j \epsilon_m P_n^{-m}(\cos \theta) P_j^{-m}(\cos \theta) \\ & \quad \cdot (n-m+1)(j-m+1) \mathcal{P}_{n+1, j+1, m} \\ & + \sum_{n=2}^{\infty} \sum_{j=1}^{n-1} \delta_{n+j, \text{odd}} [T_n T_j^* + T_j T_n^*] \sum_{m=0}^{j-1} \epsilon_m P_n^{-m}(\cos \theta) P_j^{-m}(\cos \theta) \\ & \quad \cdot (n-m+1)(j+m) \mathcal{P}_{n+1, j-1, m} \\ & + \sum_{n=1}^{\infty} \sum_{j=0}^{n-1} \delta_{n+j, \text{odd}} [T_n T_j^* + T_j T_n^*] \sum_{m=0}^j \epsilon_m P_n^{-m}(\cos \theta) P_j^{-m}(\cos \theta) \\ & \quad \cdot (n+m)(j-m+1) \mathcal{P}_{n-1, j+1, m} \\ & + \sum_{n=2}^{\infty} \sum_{j=1}^{n-1} \delta_{n+j, \text{odd}} [T_n T_j^* + T_j T_n^*] \sum_{m=0}^{j-1} \epsilon_m P_n^{-m}(\cos \theta) P_j^{-m}(\cos \theta) \\ & \quad \cdot (n+m)(j+m) \mathcal{P}_{n-1, j-1, m} \end{aligned} \right\} \quad (71)
\end{aligned}$$

Dividing Eq. 71 by Eq. 70 yields the proper expression for the signal-to-noise ratio for a circumferentially symmetric cosine squared directivity.

NUMERICAL SIMULATIONS

As with the cylinders, we have plotted $10 \log[\langle |p_s|^2 \rangle / \langle |p_N|^2 \rangle]$ with respect to azimuthal angle for a rigid sphere in a circumferentially symmetric noise field. We use the same coefficients of the cosine squared directivity so that $\alpha = 0.33/75.4$, $\beta = 1.0/75.4$, and $\gamma = 33.0/75.4$. It should be noted that these values of α , β , and γ result in a normalized noise condition which reduces Eq. 70 to unity. Our numerical simulations were carried out using the MATLAB program `sph_rig_dir` which is in Appendix F. The simulations are for ka values of 5, 20, and 40 respectively and kR values of $16ka$ and $32ka$.

In Figs. 4, 5, and 6, all solid lines indicate the function evaluated at $kR = 16 * ka$ while dashed lines indicate an evaluation of the function at $kR = 32 * ka$. For high ka , the decrease in horizontal scattering ($\theta = \pi/2$) becomes more pronounced and the forward scattering from $\theta = 0$ is greater than the backscattering from the same direction. In each figure it is also seen that the difference between the $16*ka$ case and the $32*ka$ case is on the order of 6 dB as would be expected when comparing spherical scattering at distances which differ by a factor of two.

CONCLUSION

An expression was obtained for the signal-to-noise ratio due to scattering from an infinite rigid cylinder or an infinite elastic cylindrical shell subjected to a normally incident ambient noise field. This solution is applied to the specific case of isotropic fields and to the case of noise fields which can be expressed by a squared cosine function. Similar methods were also applied to obtain the signal-to-noise ratio due to the scattering from a rigid sphere subjected to such a noise field with the assumption of circumferential symmetry.

The effect of the ambient field is to smooth the scattering function which results from a

single incident plane wave. There is still a larger forward scattering than back scattering, but the typical lobes observed from one incident plane wave are no longer distinguishable due to the contributions from all the directions.

The limitations of these results arise from the assumption that the noise field in the cylindrical case is assumed to be normally incident to the cylindrical surface. It is expected that similar procedures can be applied to obtain results for a more realistic situation. It is also expected that similar mathematical techniques can be applied to other directivity functions and to the case of an elastic spherical shell.

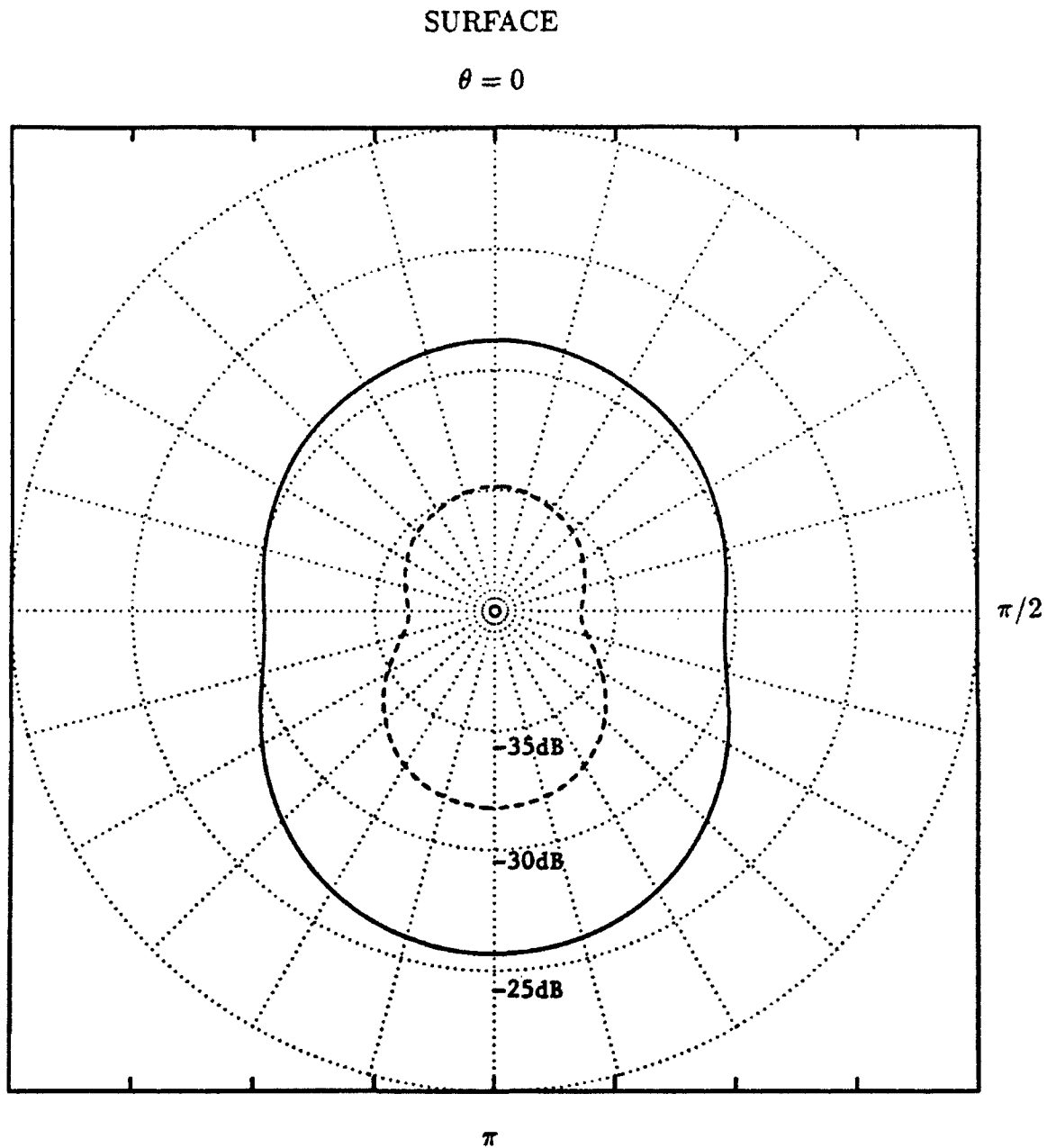


Fig. 5. $10 \log[\langle |p_s|^2 \rangle / \langle |p_N|^2 \rangle]$ for a rigid sphere evaluated at $ka = 5$. The solid line corresponds to $kR = 16 * ka$ and the dashed line corresponds to $kR = 32 * ka$.

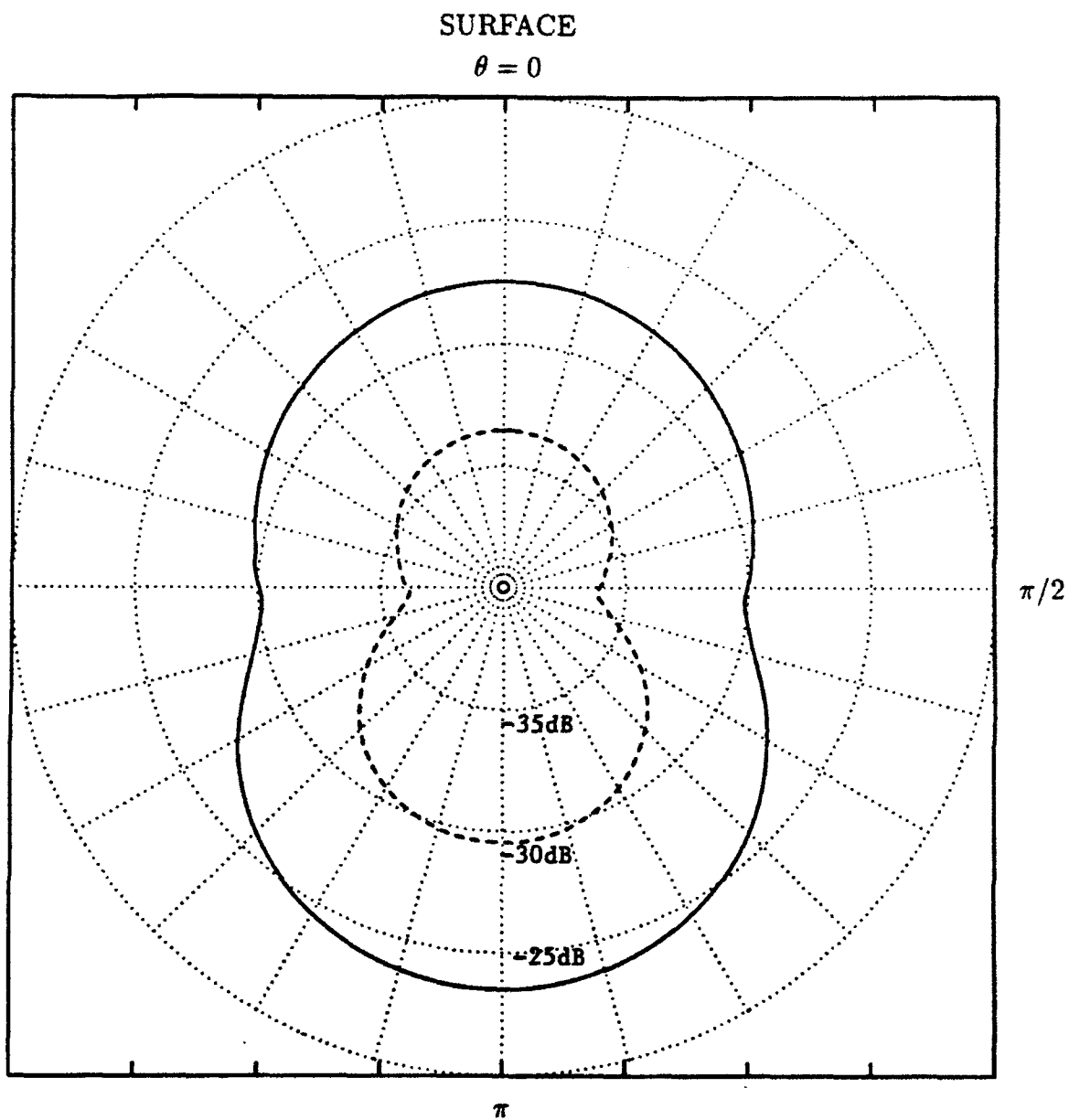


Fig. 6. $10 \log[(|p_s|^2)/(|p_N|^2)]$ for a rigid sphere evaluated at $ka = 20$.
The solid line corresponds to $kR = 16 * ka$ and the dashed line
corresponds to $kR = 32 * ka$.

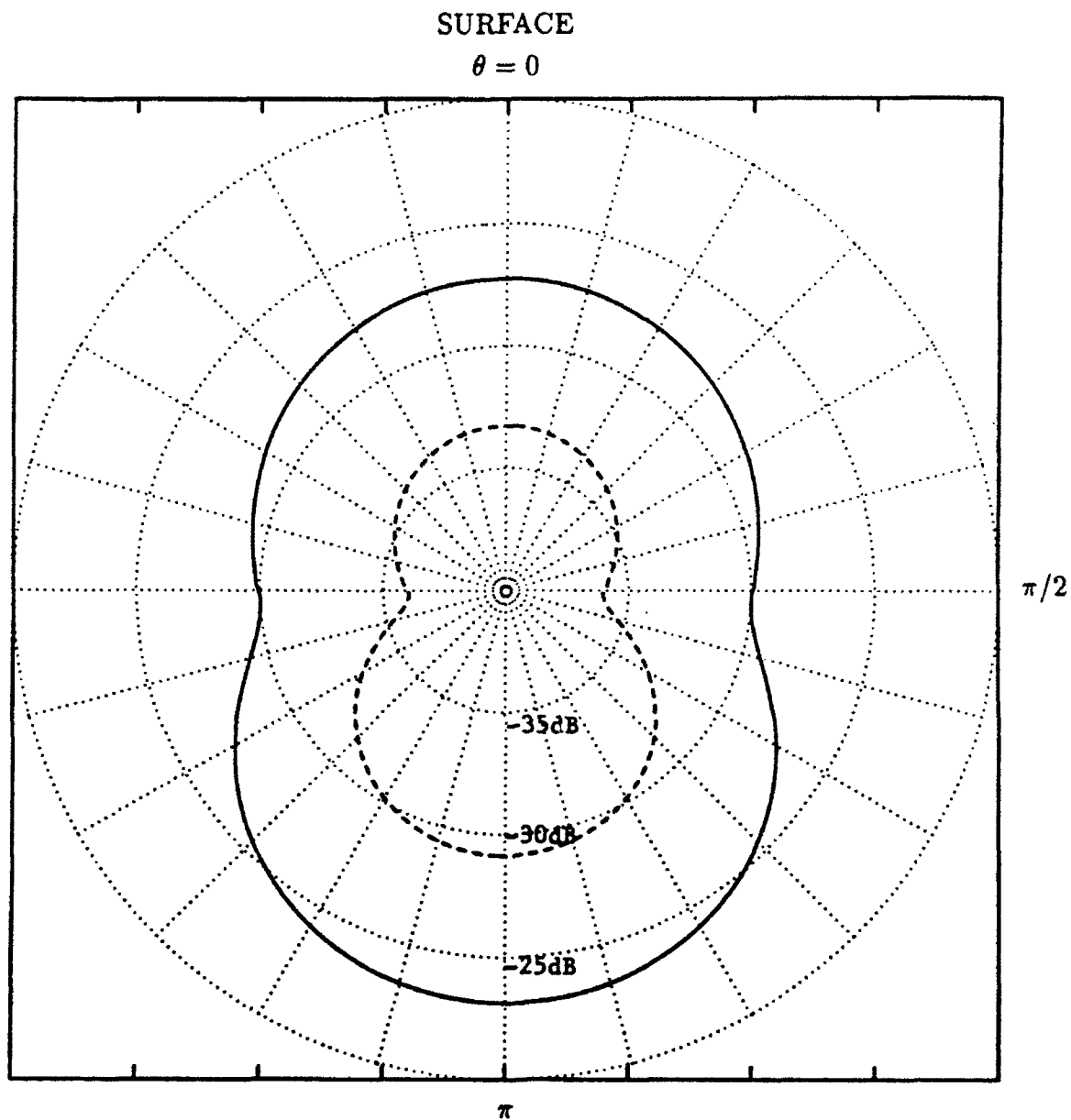


Fig. 7. $10 \log[\langle |p_s|^2 \rangle / \langle |p_N|^2 \rangle]$ for a rigid sphere evaluated at $ka = 40$.
The solid line corresponds to $kR = 16 * ka$ and the dashed line
corresponds to $kR = 32 * ka$.

APPENDIX A

MATHEMATICAL IDENTITIES

INTEGRALS OF $e^{i\eta\phi}$

$$\int_0^{2\pi} e^{i\eta\phi'} d\phi' = 2\pi\delta_{\eta,0}, \quad (72)$$

$$\int_{-\pi/2}^{\pi/2} e^{i\eta\phi'} d\phi' = \pi\delta_{\eta,0} + \frac{2}{\eta}(-1)^{(\eta-1)/2}\delta_{\eta,odd}, \quad (73)$$

and

$$\int_{\pi/2}^{3\pi/2} e^{i\eta\phi'} d\phi' = \pi\delta_{\eta,0} - \frac{2}{\eta}(-1)^{(\eta-1)/2}\delta_{\eta,odd}. \quad (74)$$

PROPERTIES OF ASSOCIATED LEGENDRE FUNCTIONS⁷

$$\begin{aligned} P_n(\cos \psi) &= P_n(\cos \theta \cos \theta' + \sin \theta \sin \theta' \cos(\phi - \phi')) \\ &= \sum_{m=0}^n \epsilon_m \frac{(n-m)!}{(n+m)!} P_n^m(\cos \theta) P_n^m(\cos \theta') \cos[m(\phi - \phi')], \end{aligned} \quad (75)$$

where P_n^m are the associated Legendre functions defined by

$$P_n^m(x) = (-1)^m (1-x^2)^{m/2} \frac{d^m}{dx^m} P_n(x), \quad (76)$$

and ϵ_m indicates the Neumann function defined by

$$\epsilon_m = \begin{cases} 1, & \text{if } m=0; \\ 2, & \text{otherwise.} \end{cases} \quad (77)$$

$$P_n^m(-x) = (-1)^{n+m} P_n^m(x), \quad (78)$$

$$\int_{-1}^1 P_n^m(x) P_j^m(x) dx = \frac{2}{(2n+1)} \frac{(n+m)!}{(n-m)!} \delta_{n,j}, \quad (79)$$

$$x P_n^m(x) = \frac{1}{(2n+1)} [(n-m+1) P_{n+1}^m(x) + (n+m) P_{n-1}^m(x)], \quad (80)$$

and

$$(-1)^m \frac{(n-m)!}{(n+m)!} P_n^m(x) = P_n^{-m}(x). \quad (81)$$

APPENDIX B

EVALUATION OF THE SCATTERED PRESSURE DUE TO A CYLINDER IN AN AMBIENT FIELD WITH A GENERAL DIRECTIONAL DIRECTIVITY

The integrations of Eqs. 34 and 35 can be evaluated using Eqs. 73 and 74 of Appendix A.

Applying these to Eq. 34 with $\eta = m$ results in

$$\begin{aligned} \frac{\langle |p_N|^2 \rangle}{|P_I|^2} &= \sum_{m=-\infty}^{\infty} a_m \left(\pi \delta_{m,0} + 2 \frac{(-1)^{(m-1)/2}}{m} \delta_{m,odd} \right) \\ &\quad + \sum_{m=-\infty}^{\infty} b_m \left(\pi \delta_{m,0} - 2 \frac{(-1)^{(m-1)/2}}{m} \delta_{m,odd} \right) \\ &= \pi(a_0 + b_0) + 2 \sum_{m=-\infty}^{\infty} (a_m - b_m) \frac{(-1)^{(m-1)/2}}{m} \delta_{m,odd}. \end{aligned} \quad (82)$$

Applying the same equations to Eq. 35 with $\eta = n - r + m$ yields

$$\begin{aligned} \frac{\langle |p_s|^2 \rangle}{|P_I|^2} &= \sum_{n=-\infty}^{\infty} \sum_{r=-\infty}^{\infty} T_n T_r^* e^{-i(n-r)\phi} \\ &\quad \cdot \left[\sum_{m=-\infty}^{\infty} a_m \left(\pi \delta_{n-r+m,0} + 2 \frac{(-1)^{(n-r+m-1)/2}}{n-r+m} \delta_{n-r+m,odd} \right) \right. \\ &\quad \left. + \sum_{m=-\infty}^{\infty} b_m \left(\pi \delta_{n-r+m,0} - 2 \frac{(-1)^{(n-r+m-1)/2}}{n-r+m} \delta_{n-r+m,odd} \right) \right]. \end{aligned} \quad (83)$$

Using the fact that $\delta_{n-r+m,0} = \delta_{n-r,-m}$, Eq. 83 simplifies to

$$\begin{aligned} \frac{\langle |p_s|^2 \rangle}{|P_I|^2} &= \pi \sum_{m=-\infty}^{\infty} (a_m + b_m) e^{im\phi} \sum_{n=-\infty}^{\infty} T_n T_{n+m}^* \\ &\quad + 2 \sum_{m=-\infty}^{\infty} (a_m - b_m) \sum_{n=-\infty}^{\infty} \sum_{r=-\infty}^{\infty} T_n T_r^* \\ &\quad \cdot \frac{e^{-i(n-r)\phi} (-1)^{(n-r+m-1)/2}}{(n-r+m)} \delta_{n-r+m,odd}. \end{aligned} \quad (84)$$

THIS PAGE INTENTIONALLY LEFT BLANK

APPENDIX C

EVALUATION OF THE SCATTERED PRESSURE FROM A RIGID SPHERE DUE TO A GENERAL CIRCUMFERENTIALLY SYMMETRIC DIRECTIVITY

As a result of circumferential symmetry, I can be separated in the following manner.

$$I(n, m, j, k) = I_{\theta'}(n, m, j, k) \cdot I_{\phi'}(m, k) \quad (85)$$

where

$$I_{\theta'}(n, m, j, k) = \int_0^\pi \sin \theta' P_n^m(\cos \theta') P_j^k(\cos \theta') \mathcal{D}(\theta') d\theta' \quad (86)$$

and

$$I_{\phi'}(m, k) = \int_0^{2\pi} \cos[m(\phi - \phi')] \cos[k(\phi - \phi')] d\phi'. \quad (87)$$

Rewriting the integrand of $I_{\phi'}(m, k)$ as

$$\cos[m(\phi - \phi')] \cos[k(\phi - \phi')] = \frac{1}{4} \sum_{\xi} e^{i\xi\phi} e^{-i\xi\phi'}, \quad (88)$$

where

$$\xi = \{m + k, -(m + k), m - k, -(m - k)\} \quad (89)$$

and applying Eq. 72 of Appendix A yields

$$\begin{aligned} I_{\phi'}(m, k) &= \frac{1}{4} \sum_{\xi} e^{i\xi\phi} \int_0^{2\pi} e^{-i\xi\phi'} d\phi' \\ &= \frac{\pi}{2} (\delta_{(m+k),0} + \delta_{-(m+k),0} + \delta_{(m-k),0} + \delta_{-(m-k),0}) \\ &= \pi (\delta_{m,0} \delta_{k,0} + \delta_{m,k}). \end{aligned} \quad (90)$$

Therefore, for a circumferentially symmetric noise field, the scattered field from a rigid sphere is obtained by applying this separation to Eqs. 62 and 63. The result is

$$\begin{aligned}
\frac{\langle |p_s(R, \theta, \phi)|^2 \rangle}{|P_I|^2} &= \pi \sum_{n=0}^{\infty} \sum_{j=0}^{\infty} \chi_{n,0} \chi_{j,0}^* P_n(\cos \theta) P_j(\cos \theta) I_{\theta'}(n, 0, j, 0) \\
&\quad + \pi \sum_{n=0}^{\infty} \sum_{j=0}^{\infty} \sum_{m=0}^{\min[n,j]} \epsilon_m^2 \chi_{n,m} \chi_{j,m}^* P_n^m(\cos \theta) P_j^m(\cos \theta) I_{\theta'}(n, m, j, m) \quad (91) \\
&= 2\pi \sum_{n=0}^{\infty} \sum_{j=0}^{\infty} \sum_{m=0}^{\min[n,j]} \epsilon_m \chi_{n,m} \chi_{j,m}^* P_n^m(\cos \theta) P_j^m(\cos \theta) I_{\theta'}(n, m, j, m).
\end{aligned}$$

Rewriting this in terms of T_n

$$\frac{\langle |p_s(R, \theta, \phi)|^2 \rangle}{|P_I|^2} = 2\pi \sum_{n=0}^{\infty} \sum_{j=0}^{\infty} (2n+1)(2j+1) T_n T_j^* \sum_{m=0}^{\min[n,j]} S_{n,j,m}, \quad (92)$$

where

$$S_{n,j,m} = \epsilon_m \frac{(n-m)!(j-m)!}{(n+m)!(j+m)!} P_n^m(\cos \theta) P_j^m(\cos \theta) I_{\theta'}(n, m, j, m). \quad (93)$$

APPENDIX D
 INTEGRATION OF TWO ASSOCIATED LEGENDRE FUNCTIONS
 OVER AN ARBITRARY RANGE CONTAINED IN $[-1, 1]$

Consider the integral⁷

$$\int_{-1}^1 P_n^m(x) P_j^m(x) dx = \frac{2}{2n+1} \frac{(n+m)!}{(n-m)!} \delta_{n,j}. \quad (94)$$

where $m \leq n$ and $m \leq j$. This is a well known integral, but when the integration limits are different, the integration is not as easily determined. Therefore, we have derived an expression for general integration limits.

The Associated Legendre functions satisfy the differential equation⁵

$$(1-x^2)y'' - 2xy' + \left\{ n(n+1) - \frac{m}{1-x^2} \right\} y = 0 \quad (95)$$

which is equivalent to

$$\frac{d}{dx} \{ (1-x^2)y' \} + \left\{ n(n+1) - \frac{m}{1-x^2} \right\} y = 0. \quad (96)$$

Multiplying by $(1-x^2)$ and substituting P_n^m and P_j^m for y , Eq. 96 becomes

$$(1-x^2) \frac{d}{dx} \{ (1-x^2) P_n^{m'} \} + \{ (1-x^2)n(n+1) - m \} P_n^m = 0 \quad (97)$$

and

$$(1-x^2) \frac{d}{dx} \{ (1-x^2) P_j^{m'} \} + \{ (1-x^2)j(j+1) - m \} P_j^m = 0, \quad (98)$$

where the primes indicate derivatives with respect to x and the argument, x , of P_n^m and P_j^m is suppressed. Multiplying Eqs. 97 and 98 by P_j^m and P_n^m respectively yields

$$(1-x^2) \frac{d}{dx} \left\{ (1-x^2) P_n^{m'} \right\} P_j^m + \{ (1-x^2) n(n+1) - m \} P_n^m P_j^m = 0 \quad (99)$$

and

$$(1-x^2) \frac{d}{dx} \left\{ (1-x^2) P_j^{m'} \right\} P_n^m + \{ (1-x^2) j(j+1) - m \} P_j^m P_n^m = 0. \quad (100)$$

When j and n are different, we subtract Eq. 100 from Eq. 99 and factor the $(1-x^2)$ term to obtain

$$\frac{d}{dx} \left\{ (1-x^2) P_n^{m'} \right\} P_j^m - \frac{d}{dx} \left\{ (1-x^2) P_j^{m'} \right\} P_n^m = \{ j(j+1) - n(n+1) \} P_j^m P_n^m. \quad (101)$$

An application of the chain rule to the quantities $(1-x^2) P_{(n,j)}^{m'}(x) P_{(j,n)}^m(x)$ yields

$$\frac{d}{dx} \left\{ (1-x^2) P_n^{m'} P_j^m \right\} = P_j^m \frac{d}{dx} \left\{ (1-x^2) P_n^{m'} \right\} + (1-x^2) P_n^{m'} P_j^{m'} \quad (102)$$

and

$$\frac{d}{dx} \left\{ (1-x^2) P_n^m P_j^{m'} \right\} = P_n^m \frac{d}{dx} \left\{ (1-x^2) P_j^{m'} \right\} + (1-x^2) P_j^{m'} P_n^{m'}. \quad (103)$$

Upon subtracting these equations we obtain

$$\begin{aligned} \frac{d}{dx} \left\{ (1-x^2) P_n^{m'} P_j^m \right\} - \frac{d}{dx} \left\{ (1-x^2) P_n^m P_j^{m'} \right\} = \\ P_j^m \frac{d}{dx} \left\{ (1-x^2) P_n^{m'} \right\} - P_n^m \frac{d}{dx} \left\{ (1-x^2) P_j^{m'} \right\}. \end{aligned} \quad (104)$$

Substituting Eq. 104 into Eq. 101 yields

$$\frac{d}{dx} \left\{ (1-x^2) [P_n^{m'} P_j^m - P_n^m P_j^{m'}] \right\} = \{j(j+1) - n(n+1)\} P_j^m P_n^m. \quad (105)$$

Integrating this equation over the interval $[a, b]$ which is contained in the interval $[-1, 1]$ yields

$$\int_a^b P_n^m(x) P_j^m(x) dx = (1-x^2) \frac{[P_n^{m'}(x) P_j^m(x) - P_n^m(x) P_j^{m'}(x)] \Big|_a^b}{j(j+1) - n(n+1)} \quad (106)$$

as a general expression for the integral of the product of associated Legendre functions. When $a = 0$ and $b = 1$ this reduces to

$$\int_0^1 P_n^m(x) P_j^m(x) dx = \frac{[P_n^m(0) P_j^{m'}(0) - P_n^{m'}(0) P_j^m(0)]}{j(j+1) - n(n+1)} \quad (107)$$

It should be noted that this integration is true for $m \leq n$ and $m \leq j$. If $m > n$ or $m > j$, then the integral is zero. It should also be noted that when $n = j$, Eqs. 99 and 100 are the same. If they were subtracted to obtain Eq. 101, the resulting equation would be $0 = 0$. Therefore when $n = j$ the integral must be evaluated in a different manner.

The integrand of Eq. 94 is even so that

$$\int_0^1 P_n^m(x) P_n^m(x) dx = \frac{1}{2n+1} \frac{(n+m)!}{(n-m)!}. \quad (108)$$

Also, for $n \neq j$ Eq. 94 can be rewritten as

$$\int_{-1}^1 P_n^m(x) P_j^m(x) dx = [1 + (-1)^{n+j}] \int_0^1 P_n^m(x) P_j^m(x) dx = 0. \quad (109)$$

Therefore when $n + j$ is an even number

$$\int_0^1 P_n^m(x) P_j^m(x) dx = 0. \quad (110)$$

Using these facts, Eq. 107 can be rewritten more precisely as

$$\int_0^1 P_n^m(x) P_j^m(x) dx = \frac{1}{(2n+1)} \frac{(n+m)!}{(n-m)!} \delta_{n,j} U_{m,n} + \mathcal{P}_{n,j,m} \delta_{n+j, \text{odd}} U_{m,n} U_{m,j}, \quad (111)$$

where

$$\mathcal{P}_{n,j,m} = \frac{P_n^m(0) P_j^{m'}(0) - P_n^{m'}(0) P_j^m(0)}{j(j+1) - n(n+1)}, \quad (112)$$

and

$$U_{m,M} = \begin{cases} 1, & 0 \leq m \leq M; \\ 0, & \text{otherwise.} \end{cases} \quad (113)$$

APPENDIX E

EVALUATION OF THE SCATTERED PRESSURE FROM A RIGID SPHERE DUE TO A CIRCUMFERENTIALLY SYMMETRIC SURFACE NOISE DIRECTIVITY

Applying Eq. 69 to Eq. 67 reduces the integral term for the scattered pressure to

$$\begin{aligned}
 I_{\theta'}(n, m, j, m) &= \alpha \int_0^{\pi} \sin(\theta') P_n^m(\cos \theta') P_j^m(\cos \theta') d\theta' \\
 &\quad + \beta \int_0^{\pi/2} \sin(\theta') \cos^2(\theta') P_n^m(\cos \theta') P_j^m(\cos \theta') d\theta' \\
 &\quad + \gamma \int_{\pi/2}^{\pi} \sin(\theta') \cos^2(\theta') P_n^m(\cos \theta') P_j^m(\cos \theta') d\theta' \\
 &= \alpha \int_{-1}^1 P_n^m(x) P_j^m(x) dx + [\beta + (-1)^{n+j} \gamma] \int_0^1 x^2 P_n^m(x) P_j^m(x) dx
 \end{aligned} \tag{114}$$

The latter expression is obtained using the substitutions $x = \cos(\theta')$, $dx = -\sin(\theta') d\theta'$, and applying Eq. 78 of Appendix A. For the first integration, apply the orthogonality relation of Associated Legendre functions as given in Eq. 79 of Appendix A, and in the second integral, apply the identity given in Eq. 80 to $x P_n^m(x)$ and $x P_j^m(x)$. The second integral therefore becomes

$$\begin{aligned}
 \int_0^1 x^2 P_n^m(x) P_j^m(x) dx &= \\
 \frac{1}{(2n+1)(2j+1)} &\left\{ \begin{aligned} &(n-m+1)(j-m+1) \int_0^1 P_{n+1}^m(x) P_{j+1}^m(x) dx \\ &+ (n-m+1)(j+m) \int_0^1 P_{n+1}^m(x) P_{j-1}^m(x) dx \\ &+ (n+m)(j-m+1) \int_0^1 P_{n-1}^m(x) P_{j+1}^m(x) dx \\ &+ (n+m)(j+m) \int_0^1 P_{n-1}^m(x) P_{j-1}^m(x) dx \end{aligned} \right\}.
 \end{aligned} \tag{115}$$

In Appendix D it was shown that,

$$\int_0^1 P_n^m(x) P_j^m(x) dx = \frac{1}{(2n+1)} \frac{(n+m)!}{(n-m)!} \delta_{n,j} U_{m,n} + \mathcal{P}_{n,j,m} \delta_{n+j, \text{odd}} U_{m,n} U_{m,j}. \quad (116)$$

When this is applied to the integrations of Eq. 115, the second integral of Eq. 114 becomes

$$\int_0^1 x^2 P_n^m(x) P_j^m(x) dx = \frac{1}{(2n+1)(2j+1)} \left\{ \begin{aligned} & (n-m+1)(j-m+1) \mathcal{P}_{n+1,j+1,m} \delta_{n+j+2, \text{odd}} U_{m,n+1} U_{m,j+1} \\ & + (n-m+1)(j+m) \mathcal{P}_{n+1,j-1,m} \delta_{n+j, \text{odd}} U_{m,n+1} U_{m,j-1} \\ & + (n+m)(j-m+1) \mathcal{P}_{n-1,j+1,m} \delta_{n+j, \text{odd}} U_{m,n-1} U_{m,j+1} \\ & + (n+m)(j+m) \mathcal{P}_{n-1,j-1,m} \delta_{n+j-2, \text{odd}} U_{m,n-1} U_{m,j-1}. \end{aligned} \right\} \quad (117)$$

$$+ \frac{1}{(2n+1)(2j+1)} \left\{ \begin{aligned} & \frac{(n-m+1)(j-m+1)}{(2n+3)} \frac{(n+m+1)!}{(n-m+1)!} \delta_{n+1,j+1} U_{m,n+1} \\ & + \frac{(n-m+1)(j+m)}{(2n+3)} \frac{(n+m+1)!}{(n-m+1)!} \delta_{n+1,j-1} U_{m,n+1} \\ & + \frac{(n+m)(j-m+1)}{(2n-1)} \frac{(n+m-1)!}{(n-m-1)!} \delta_{n-1,j+1} U_{m,n-1} \\ & + \frac{(n+m)(j+m)}{(2n-1)} \frac{(n+m-1)!}{(n-m-1)!} \delta_{n-1,j-1} U_{m,n-1} \end{aligned} \right\}$$

Applying this and the delta function identities $\delta_{n\pm 1,j\pm 1} = \delta_{n,j}$, $\delta_{n\pm 1,j\mp 1} = \delta_{n\pm 2,j}$, and

$\delta_{n+j\pm 2, \text{odd}} = \delta_{n+j, \text{odd}}$ reduces $I_{\theta'}$ to

$$I_{\theta'}(n, m, j, m) = \alpha \frac{2}{(2n+1)} \frac{(n+m)!}{(n-m)!} \delta_{n,j}$$

$$+ \frac{[\beta + \gamma]}{(2n+1)(2j+1)} \left\{ \begin{aligned} & \frac{(j-m+1)}{(2n+3)} \frac{(n+m+1)!}{(n-m)!} \delta_{n,j} U_{m,n+1} \\ & + \frac{(j+m)}{(2n+3)} \frac{(n+m+1)!}{(n-m)!} \delta_{n+2,j} U_{m,n+1} \\ & + \frac{(j-m+1)}{(2n-1)} \frac{(n+m)!}{(n-m-1)!} \delta_{n-2,j} U_{m,n-1} \\ & + \frac{(j+m)}{(2n-1)} \frac{(n+m)!}{(n-m-1)!} \delta_{n,j} U_{m,n-1} \end{aligned} \right\} \quad (118)$$

$$+ \frac{[\beta - \gamma] \delta_{n+j, \text{odd}}}{(2n+1)(2j+1)} \left\{ \begin{aligned} & (n-m+1)(j-m+1) \mathcal{P}_{n+1,j+1,m} U_{m,n+1} U_{m,j+1} \\ & + (n-m+1)(j+m) \mathcal{P}_{n+1,j-1,m} U_{m,n+1} U_{m,j-1} \\ & + (n+m)(j-m+1) \mathcal{P}_{n-1,j+1,m} U_{m,n-1} U_{m,j+1} \\ & + (n+m)(j+m) \mathcal{P}_{n-1,j-1,m} U_{m,n-1} U_{m,j-1} \end{aligned} \right\}$$

Substituting this expression into Eqs. 66 and 68 yields

$$\begin{aligned}
\frac{\langle |p_s(R, \theta, \phi)|^2 \rangle}{|P_I|^2} &= 4\pi\alpha \sum_{n=0}^{\infty} (2n+1) T_n T_n^* \sum_{m=0}^n \epsilon_m \frac{(n-m)!}{(n+m)!} P_n^m(\cos \theta) P_n^m(\cos \theta) \\
&+ \pi[\beta + \gamma] \sum_{n=0}^{\infty} \sum_{j=0}^n \epsilon_{(n-j)} [T_n T_j^* + T_j T_n^*] \\
&\cdot \sum_{m=0}^j \epsilon_m \frac{(n-m)!}{(n+m)!} \frac{(j-m)!}{(j+m)!} P_n^m(\cos \theta) P_j^m(\cos \theta) \\
&\cdot \left\{ \begin{aligned} &\frac{(j-m+1)(n+m+1)!}{(2n+3)(n-m)!} \delta_{n,j} U_{m,n+1} \\ &+ \frac{(j+m)(n+m+1)!}{(2n+3)(n-m)!} \delta_{n+2,j} U_{m,n+1} \\ &+ \frac{(j-m+1)(n+m)!}{(2n-1)(n-m-1)!} \delta_{n-2,j} U_{m,n-1} \\ &+ \frac{(j+m)(n+m)!}{(2n-1)(n-m-1)!} \delta_{n,j} U_{m,n-1} \end{aligned} \right\} \quad (119) \\
&+ \pi[\beta - \gamma] \sum_{n=0}^{\infty} \sum_{j=0}^n \delta_{n+j, \text{odd}} \epsilon_{(n-j)} [T_n T_j^* + T_j T_n^*] \\
&\cdot \sum_{m=0}^j \epsilon_m \frac{(n-m)!}{(n+m)!} \frac{(j-m)!}{(j+m)!} P_n^m(\cos \theta) P_j^m(\cos \theta) \\
&\cdot \left\{ \begin{aligned} &(n-m+1)(j-m+1) \mathcal{P}_{n+1,j+1,m} U_{m,n+1} U_{m,j+1} \\ &+ (n-m+1)(j+m) \mathcal{P}_{n+1,j-1,m} U_{m,n+1} U_{m,j-1} \\ &+ (n+m)(j-m+1) \mathcal{P}_{n-1,j+1,m} U_{m,n-1} U_{m,j+1} \\ &+ (n+m)(j+m) \mathcal{P}_{n-1,j-1,m} U_{m,n-1} U_{m,j-1} \end{aligned} \right\}
\end{aligned}$$

Note that whenever $n + j$ is odd, $\epsilon_{n-j} = 2$, $(-1)^{n+j} = -1$ and the limits $n = [0, \infty]$, $j = [0, n]$ can be replaced by $n = [1, \infty]$, $j = [0, n - 1]$. Using these identities, applying Eq. 81 of Appendix A to the $\beta \pm \gamma$ terms, and applying Eq. 75 of Appendix A to the α term simplifies Eq. 119 to

$$\begin{aligned}
\frac{\langle |p_s|^2 \rangle}{|P_r|^2} &= 4\pi\alpha \sum_{n=0}^{\infty} (2n+1) T_n T_n^* \\
&+ \pi[\beta + \gamma] \sum_{n=0}^{\infty} \sum_{j=0}^n \epsilon_{(n-j)} [T_n T_j^* + T_j T_n^*] \sum_{m=0}^j \epsilon_m P_n^{-m}(\cos \theta) P_j^{-m}(\cos \theta) \\
&\quad \left\{ \begin{aligned} &\frac{(j-m+1)(n+m+1)!}{(2n+3)(n-m)!} \delta_{n,j} U_{m,n+1} \\ &+ \frac{(j+m)(n+m+1)!}{(2n+3)(n-m)!} \delta_{n+2,j} U_{m,n+1} \\ &+ \frac{(j-m+1)(n+m)!}{(2n-1)(n-m-1)!} \delta_{n-2,j} U_{m,n-1} \\ &+ \frac{(j+m)(n+m)!}{(2n-1)(n-m-1)!} \delta_{n,j} U_{m,n-1} \end{aligned} \right\} \quad (120) \\
&+ 2\pi[\beta - \gamma] \sum_{n=1}^{\infty} \sum_{j=0}^{n-1} \delta_{n+j, \text{odd}} [T_n T_j^* + T_j T_n^*] \sum_{m=0}^j \epsilon_m P_n^{-m}(\cos \theta) P_j^{-m}(\cos \theta) \\
&\quad \left\{ \begin{aligned} &(n-m+1)(j-m+1) \mathcal{P}_{n+1,j+1,m} U_{m,n+1} U_{m,j+1} \\ &+ (n-m+1)(j+m) \mathcal{P}_{n+1,j-1,m} U_{m,n+1} U_{m,j-1} \\ &+ (n+m)(j-m+1) \mathcal{P}_{n-1,j+1,m} U_{m,n-1} U_{m,j+1} \\ &+ (n+m)(j+m) \mathcal{P}_{n-1,j-1,m} U_{m,n-1} U_{m,j-1} \end{aligned} \right\}
\end{aligned}$$

Eliminating the delta functions and step functions yields an average scattered pressure of

$$\begin{aligned}
\frac{\langle |p_s|^2 \rangle}{|P_i|^2} &= 4\pi\alpha \sum_{n=0}^{\infty} (2n+1) T_n T_n^* \\
&+ 2\pi(\beta + \gamma) \cdot \left\{ \begin{aligned} &\sum_{n=0}^{\infty} [T_n T_n^*] \sum_{m=0}^n \epsilon_m P_n^{-m}(\cos \theta) P_n^{-m}(\cos \theta) \frac{(n-m+1)(n+m+1)!}{(2n+3)(n-m)!} \\ &+ \sum_{n=2}^{\infty} [T_n T_{n-2}^* + T_{n-2} T_n^*] \\ &\quad \cdot \sum_{m=0}^{n-2} \epsilon_m P_n^{-m}(\cos \theta) P_{n-2}^{-m}(\cos \theta) \frac{1}{(2n-1)} \frac{(n+m)!}{(n-m-2)!} \\ &+ \sum_{n=1}^{\infty} [T_n T_n^*] \sum_{m=0}^{n-1} \epsilon_m P_n^{-m}(\cos \theta) P_n^{-m}(\cos \theta) \frac{(n+m)}{(2n-1)} \frac{(n+m)!}{(n-m-1)!} \end{aligned} \right\} \\
&+ 2\pi(\beta - \gamma) \cdot \left\{ \begin{aligned} &\sum_{n=1}^{\infty} \sum_{j=0}^{n-1} \delta_{n+j, \text{odd}} [T_n T_j^* + T_j T_n^*] \sum_{m=0}^j \epsilon_m P_n^{-m}(\cos \theta) P_j^{-m}(\cos \theta) \\ &\quad \cdot (n-m+1)(j-m+1) \mathcal{P}_{n+1, j+1, m} \\ &+ \sum_{n=2}^{\infty} \sum_{j=1}^{n-1} \delta_{n+j, \text{odd}} [T_n T_j^* + T_j T_n^*] \sum_{m=0}^{j-1} \epsilon_m P_n^{-m}(\cos \theta) P_j^{-m}(\cos \theta) \\ &\quad \cdot (n-m+1)(j+m) \mathcal{P}_{n+1, j-1, m} \\ &+ \sum_{n=1}^{\infty} \sum_{j=0}^{n-1} \delta_{n+j, \text{odd}} [T_n T_j^* + T_j T_n^*] \sum_{m=0}^j \epsilon_m P_n^{-m}(\cos \theta) P_j^{-m}(\cos \theta) \\ &\quad \cdot (n+m)(j-m+1) \mathcal{P}_{n-1, j+1, m} \\ &+ \sum_{n=2}^{\infty} \sum_{j=1}^{n-1} \delta_{n+j, \text{odd}} [T_n T_j^* + T_j T_n^*] \sum_{m=0}^{j-1} \epsilon_m P_n^{-m}(\cos \theta) P_j^{-m}(\cos \theta) \\ &\quad \cdot (n+m)(j+m) \mathcal{P}_{n-1, j-1, m} \end{aligned} \right\} \quad (121)
\end{aligned}$$

APPENDIX F

**MATLAB PROGRAMS FOR EVALUATING THE AMBIENT
NOISE SCATTERING FROM INFINITE RIGID AND ELASTIC
CYLINDERS AND FROM RIGID SPHERES**

```

% cyl_inf_rig_elas
%
%
% This program determines the scattering from an infinite rigid
% cylinder and an infinite elastic cylinder due to a directional
% ambient noise field described by the directivity
%    $D(\text{PHI}) = \text{Sum}[a(m) \exp(im*\text{phi})]; \quad -\pi/2 < \text{PHI} < \pi/2$ 
%    $D(\text{PHI}) = \text{Sum}[b(m) \exp(im*\text{phi})]; \quad \pi/2 < \text{PHI} < 3\pi/2.$ 
% The above directivity function is a general fourier expansion,
% and the program is written so that any directivity of this
% form can be used. Specifically
%    $D(\text{PHI}) = \alpha + \beta \cos(\text{PHI})^2; \quad -\pi/2 < \text{PHI} < \pi/2$ 
%    $D(\text{PHI}) = \alpha + \gamma \cos(\text{PHI})^2; \quad \pi/2 < \text{PHI} < 3\pi/2$ 
% is used. From this directivity function  $a(m)$  and  $b(m)$  are
%    $a(0) = \alpha + \beta/2 \quad a(2) = a(-2) = \beta/4$ 
%    $b(0) = \alpha + \gamma/2 \quad b(2) = b(-2) = \gamma/4.$ 
%
%
%
clear

% -----FOURIER COEFFICIENTS-----
alpha = 0.33/75.4;
beta = 1.0/75.4;
gamma = 33.0/75.4;
mvec = [-2 0 2]; % m for nonzero coeff.
am = [beta/4 (alpha + beta/2) beta/4]; % [a(-2) a(0) a(2)]
bm = [gamma/4 (alpha + gamma/2) gamma/4]; % [b(-2) b(0) b(2)]
apb = am + bm;
amb = am - bm;

% -----WAVENUMBER VARIABLES-----
ka = 20.0; % nondimensional wavenumber
kamult = [16 32]; % observation points are at
kR = ka*kamult; % one and two boat lengths
kRka = [kR(1) kR(2) ka];
numka = length(kRka);

```

```

% -----ANGLE VALUES-----
phimin = -pi/2.0;
phimax = 3*pi/2;
numphi = 201;
phistep = (phimax-phimin)/(numphi-1);
phi = phimin:phistep:phimax;      % angle vector

% -----ELASTICITY CONSTANTS-----
ccp = 1/3.5;                      % c/cp -- sound speed ratio
rhosrho = 7.500;                  % rhos/rho -- density ratio
ha = 1/100;                       % h/a -- thickness/radius ratio
Omega = ka*ccp;                   % nondimensional freq. parameter
betasqr = (ha^2)/12;

% -----PROGRAM PREPARATION-----
maxnr = 30;                       % sum to maxnr rather than inf.
maxm = max(abs(mvec));
iplusn(0+1) = 1;
for n = 1:maxnr+maxm
    iplusn(n+1) = i*iplusn(n);
end %for n--1
imphi = i*mvec.*phi;
eimphi = exp(imphi);

% -----BESSEL CALL-----
[J,dJ,Y,dY] = vJdJYdY(maxnr+maxm,kRka); % J(n,k)=J(n,kR(k));
H = J + i*Y;                        % J(n,numka) = J(n,ka)
dHka = dJ(:,numka) + i*dY(:,numka);   % only need H'(ka)

% -----ELASTICITY TERMS-----
for n = 0:maxnr+maxm
    nsquare(n+1) = n^2;
    nfourth(n+1) = n^4;
    nsixth(n+1) = n^6;
end %for n--2
om2n2 = Omega^2 - nsquare;
num = om2n2*2*i*ccp/pi;
den1 = Omega*H(:,numka).*om2n2.';
den2 = ha*rhosrho*dHka/ccp;

```

```

den3 = Omega^4-Omega^2*(1+nsquare+betasqr*nfourth)+betasqr*nsixth;
den = den1-den2.*den3.';
elastic = num.'./den;

```

```

% -----MAIN PROGRAM-----

```

```

for R=1:numka-1
    coeffn_r = iplusn.'.*dJ(:,numka).*H(:,R)./dHka;
    coeffr_r = conj(coeffn_r);
    coeffn_e = iplusn.'*(dJ(:,numka)+elastic).*H(:,R)./dHka;
    coeffr_e = conj(coeffn_e);

    sumlm_r = zeros(phi);
    sumlm_e = zeros(phi);
    for j = 1:length(mvec)
        m = mvec(j);
        sumn_r = 0;
        sumn_e = 0;
        for n = -maxnr:maxnr
            sumn_r = sumn_r + coeffn_r(abs(n)+1)*coeffr_r(abs(n+m)+1);
            sumn_e = sumn_e + coeffn_e(abs(n)+1)*coeffr_e(abs(n+m)+1);
        end %for n--3
        sumlm_r = sumlm_r + apb(j)*eimphi(j,:)*sumn_r;
        sumlm_e = sumlm_e + apb(j)*eimphi(j,:)*sumn_e;
    end %for j--1
    sumlm_r = pi*sumlm_r;
    sumlm_e = pi*sumlm_e;

    sum2m_r = zeros(phi);
    sum2m_e = zeros(phi);
    for j = 1:length(mvec)
        m = mvec(j);
        sumnr_r = zeros(phi);
        sumnr_e = zeros(phi);
        for n = -maxnr:maxnr
            for r = -maxnr:maxnr
                odd = (-1)^(n-r+m);
                if odd == -1
                    enrphi = exp(-i*(n-r)*phi);
                    chinr_r = coeffn_r(abs(n)+1)*coeffr_r(abs(r)+1);

```

```

        sumnr_r = sumnr_r + (-1)^((n-r+m-1)/2)*chinr_r*enrphi/(n-r+m);
        chinr_e = coeffn_e(abs(n)+1)*coeffr_e(abs(r)+1);
        sumnr_e = sumnr_e + (-1)^((n-r+m-1)/2)*chinr_e*enrphi/(n-r+m);
    end % if--odd
end %for r--1
end %for n--4
sum2m_r = sum2m_r + amb(j)*sumnr_r;
sum2m_e = sum2m_e + amb(j)*sumnr_e;
end %for j--2
sum2m_r = 2*sum2m_r;
sum2m_e = 2*sum2m_e;

sigtonoise_r(R,:) = (sum1m_r + sum2m_r)/(pi*apb(2));
sigtonoise_e(R,:) = (sum1m_e + sum2m_e)/(pi*apb(2));
TS_r(R,:) = 10*log10(sigtonoise_r(R,:));
TS_e(R,:) = 10*log10(sigtonoise_e(R,:));
end %for R--1
end

```

```

% sph_rig_dir
%
%
% This program determines the scattering from a rigid sphere due to a
% directional ambient noise field described by the directivity
%  $D(\text{THETA}) = \alpha + \beta \cos(\text{THETA})^2$ ;  $0 < \text{THETA} < \pi/2$ 
%  $D(\text{THETA}) = \alpha + \gamma \cos(\text{THETA})^2$ ;  $\pi/2 < \text{THETA} < \pi$ 
%
%
clear

% -----DIRECTIVITY COEFFICIENTS-----
alpha = 0.33/75.4;
beta = 1.0/75.4;
gamma = 33.0/75.4;

% -----WAVENUMBER VARIABLES-----
ka = 5.0; % nondimensional wavenumber
kamult = [16 32]; % observation points are at
kR = ka*kamult; % one and two boat lengths
kRka = [kR(1) kR(2) ka];

% -----ANGLE VALUES-----
numtheta = 101;
thetamin = 0;
thetamax = pi;
deltatheta = (thetamax - thetamin)/(numtheta - 1);
theta = thetamin:deltatheta:thetamax; % angle vector

% -----PROGRAM PREPARATION-----
maxn = 15; % sum to maxn rather than infinity
ivec(0+1)=1;
epsm(0+1) = 1;
minuslvec(0+1) = 1;
n2vec(0+1) = 1;
for n=1:maxn
    ivec(n+1) = i*ivec(n);
    minuslvec(n+1) = (-1)^n;

```

```

    n2vec(n+1) = 2*n+1;
    epsm(n+1) = 2;
end % for n--1

fact(0+1) = 1;
for n=1:2*maxn+1
    fact(n+1) = n*fact(n);
end % n--2

for n=0:maxn
    for m=0:maxn
        leg_fact_rat(n+1,m+1)=0;
        coeff2(n+1,m+1)=0;
        coeff3(n+1,m+1)=0;
        coeff4(n+1,m+1)=0;
    end % for m--1
end % for n--3
for n=0:maxn
    for m=0:n
        leg_fact_rat(n+1,m+1)=fact(n-m+1)/fact(n+m+1);
        coeff2(n+1,m+1)=2*((n-m+1)*fact(n+m+1+1))/((2*n+3)*fact(n-m+1));
        coeff3(n+1,m+1)=2*((n+m)*(n-m)*fact(n+m+1))/((2*n-1)*fact(n-m+1));
        coeff4(n+1,m+1)=2*((n-m)*(n-m-1)*fact(n+m+1))/((2*n-1)*fact(n-m+1));
    end % for m--2
end % for n--4
coeff2(:,0+1)=coeff2(:,0+1)/2;
coeff3(:,0+1)=coeff3(:,0+1)/2;
coeff4(:,0+1)=coeff4(:,0+1)/2;

for n=0:maxn+1
    for j=0:maxn+1
        P0coeff(n+1,j+1)=0;
    end % for j--1
end % for n--5

for n=0:maxn+1
    for j=n-1:-2:0
        P0coeff(n+1,j+1)=1/(j*(j+1)-n*(n+1));
    end % for j--2
end % for n--6

```

```

% -----MAIN PROGRAM-----

%-----BESSEL CALL-----
[jn djn yn dyn] = bessell_sph(maxn,kRka);
hn = jn + i*yn;
dhn = djn + i*dyn;
kappa_1 = ivec.*(djn(:,3).*hn(:,1)./dhn(:,3)).';
kappa_2 = ivec.*(djn(:,3).*hn(:,2)./dhn(:,3)).';

TnTj_1 = kappa_1.*conj(kappa_1)+conj(kappa_1.)*kappa_1;
TnTj_2 = kappa_2.*conj(kappa_2)+conj(kappa_2.)*kappa_2;
TnTn_1 = kappa_1.*conj(kappa_1);
TnTn_2 = kappa_2.*conj(kappa_2);

[P0,dP0] = LegendrePnm(maxn+1,0);

% -----SUM1-----
sum1_1=n2vec*TnTn_1.';
sum1_2=n2vec*TnTn_2.';

% ---Theta loop---
for k=1:numtheta
    [P dP] = LegendrePnm(maxn,cos(theta(k)));
    Pcos = leg_fact_rat.*P;

    % -----SUM2-----
    sum2_1=0;
    sum2_2=0;
    for n=0:maxn
        sum2m=0;
        for m=0:n
            sum2m=sum2m+Pcos(n+1,m+1)*Pcos(n+1,m+1)*coeff2(n+1,m+1);
        end %for m--sum2
        sum2_1=sum2_1+TnTn_1(n+1)*sum2m;
        sum2_2=sum2_2+TnTn_2(n+1)*sum2m;
    end %for n--sum2

```

```

% -----SUM3-----
sum3_1=0;
sum3_2=0;
for n=2:maxn
    sum3m=0;
    for m=0:n-2
        sum3m=sum3m+Pcos(n+1,m+1)*Pcos(n-2+1,m+1)*coeff3(n+1,m+1);
    end %for m--sum3
    sum3_1=sum3_1+TnTj_1(n+1,n-2+1)*sum3m;
    sum3_2=sum3_2+TnTj_2(n+1,n-2+1)*sum3m;
end %for n--sum3

% -----SUM4-----
sum4_1=0;
sum4_2=0;
for n=1:maxn
    sum4m=0;
    for m=0:n-1
        sum4m=sum4m+Pcos(n+1,m+1)*Pcos(n+1,m+1)*coeff4(n+1,m+1);
    end %for m--sum4
    sum4_1=sum4_1+TnTn_1(n+1)*sum4m;
    sum4_2=sum4_2+TnTn_2(n+1)*sum4m;
end %for n--sum4

% -----SUM5-----
sum5_1=0;
sum5_2=0;
for n = 1:maxn
    for j = n-1:-2:0
        sum5m=0;
        for m=0:j
            P0term=P0(n+1+1,m+1)*dP0(j+1+1,m+1)-dP0(n+1+1,m+1)*P0(j+1+1,m+1);
            mcoeff=epsm(m+1)*(n-m+1)*(j-m+1);
            sum5m=sum5m+Pcos(n+1,m+1)*Pcos(j+1,m+1)*mcoeff*P0term;
        end %for m--sum5
        sum5_1 = sum5_1+sum5m*TnTj_1(n+1,j+1)*P0coeff(n+1+1,j+1+1);
        sum5_2 = sum5_2+sum5m*TnTj_2(n+1,j+1)*P0coeff(n+1+1,j+1+1);
    end %for j--sum5
end %for n--sum5

```

```
% -----SUM6-----
```

```
sum6_1=0;
```

```
sum6_2=0;
```

```
for n = 2:maxn
```

```
    for j = n-1:-2:1
```

```
        sum6m=0;
```

```
        for m=0:j-1
```

```
            P0term=P0(n+1+1,m+1)*dP0(j-1+1,m+1)-dP0(n+1+1,m+1)*P0(j-1+1,m+1);
```

```
            mcoeff=epsm(m+1)*(n-m+1)*(j+m);
```

```
            sum6m=sum6m+Pcos(n+1,m+1)*Pcos(j+1,m+1)*mcoeff*P0term;
```

```
        end %for m--sum6
```

```
        sum6_1 = sum6_1+sum6m*TnTj_1(n+1,j+1)*P0coeff(n+1+1,j-1+1);
```

```
        sum6_2 = sum6_2+sum6m*TnTj_2(n+1,j+1)*P0coeff(n+1+1,j-1+1);
```

```
    end %for j--sum6
```

```
end %for n--sum6
```

```
% -----SUM7-----
```

```
sum7_1=0;
```

```
sum7_2=0;
```

```
for n = 1:maxn
```

```
    for j = n-1:-2:0
```

```
        sum7m=0;
```

```
        for m=0:j
```

```
            P0term=P0(n-1+1,m+1)*dP0(j+1+1,m+1)-dP0(n-1+1,m+1)*P0(j+1+1,m+1);
```

```
            mcoeff=epsm(m+1)*(n+m)*(j-m+1);
```

```
            sum7m=sum7m+Pcos(n+1,m+1)*Pcos(j+1,m+1)*mcoeff*P0term;
```

```
        end %for m--sum7
```

```
        sum7_1 = sum7_1+sum7m*TnTj_1(n+1,j+1)*P0coeff(n-1+1,j+1+1);
```

```
        sum7_2 = sum7_2+sum7m*TnTj_2(n+1,j+1)*P0coeff(n-1+1,j+1+1);
```

```
    end %for j--sum7
```

```
end %for n--sum7
```

```
% -----SUM8-----
```

```
sum8_1=0;
```

```
sum8_2=0;
```

```
for n = 2:maxn
```

```
    for j = n-1:-2:1
```

```
        sum8m=0;
```

```

for m=0:j-1
    P0term=P0(n-1+1,m+1)*dP0(j-1+1,m+1)-dP0(n-1+1,m+1)*P0(j-1+1,m+1);
    mcoeff=epsm(m+1)*(n+m)*(j+m);
    sum8m=sum8m+Pcos(n+1,m+1)*Pcos(j+1,m+1)*mcoeff*P0term;
end %for m--sum8
sum8_1 = sum8_1+sum8m*TnTj_1(n+1,j+1)*P0coeff(n-1+1,j-1+1);
sum8_2 = sum8_2+sum8m*TnTj_2(n+1,j+1)*P0coeff(n-1+1,j-1+1);
end %for j--sum8
end %for n--sum8

```

```

p1_1=sum1_1;
p1_2=sum1_2;
p2_1=(sum2_1+sum3_1+sum4_1);
p2_2=(sum2_2+sum3_2+sum4_2);
p3_1=(sum5_1+sum6_1+sum7_1+sum8_1);
p3_2=(sum5_2+sum6_2+sum7_2+sum8_2);
Pressure1(k)=4*pi*alpha*p1_1+2*pi*(beta+gamma)*p2_1+2*pi*(beta-gamma)*p3_1;
Pressure2(k)=4*pi*alpha*p1_2+2*pi*(beta+gamma)*p2_2+2*pi*(beta-gamma)*p3_2;
end % for theta

```

```

pn=2*pi*(2*alpha+(1/3)*(beta+gamma));
TS1=10*log10(Pressure/pn);
TS2=10*log10(Pressure2/pn);
TS(1,:)=TS1;
TS(2,:)=TS2;

```

```

end

```

THIS PAGE INTENTIONALLY LEFT BLANK

REFERENCES

1. Urick, Robert J., Principles of Underwater Sound, 3rd Ed., McGraw Hill, Inc., New York. N.Y. (1983).
2. Burdic, William S., Underwater Acoustic System Analysis, 2nd Ed., Prentice Hall, Englewood Cliffs, N.J. (1991).
3. Yam, Philip, "Sound System: Using the Ocean's Noise to Image Undersea Objects", Scientific American, (Jul 1992).
4. Junger, Miguel C., and Feit, David, Sound, Structures, and Their Interaction, 2nd Ed., MIT Press, Cambridge, Mass. (1986).
5. Abramowitz, Milton, and Stegun, Irene A., Handbook of Mathematical Functions, Dover Publications, Inc., New York, N.Y. (1972).
6. Miller, G. N., "Test Module Inputs", PSI Technical Report ATD 89-067 (May 1991)
7. Gradshteyn, I.S. and Ryzhik, I.M., Table of Integrals, Series, and Products, Academic Press, Inc., San Diego, Calif. (1980).

THIS PAGE INTENTIONALLY LEFT BLANK

INITIAL DISTRIBUTION

Copies

4	ONR
1	122 A. Tucker
1	122A2 R. Vogelsong
1	122R3 G. Main
1	233 G. Remmers
1	NAVSEA
1	1 05TC CDR Coulter
1	PEO SUB
1	1 XT3 G. Mossman
1	NUWC NLON
1	1 311 R. P. Radlinski
12	DTIC
2	Cambridge Acous. Assoc.
1	M. Junger
1	J. Garrelick

CENTER DISTRIBUTION

Copies	Code	Name
1	70	M. M. Sevik
1	701	G. Smith
1	7022	G. M. Janik
1	7023	W. K. Blake
1	7024	D. Feit
1	7025	R. J. Cantrell
1	7026	Y. N. Liu
1	7027	D. J. Vendittis
1	7035	G. M. Jebson
1	7301	J. R. Peoples
1	74	M. L. Montroll
1	7403	M. L. Rumerman
1	741	D. C. Honeycutt
8	745	J. Niemiec
	745	P. Arveson
	745	J. Dlubac
	745	R. L. Honeycutt
	745	S. Johnson
	745	K. Jones
	745	J. Maxwell
	745	S. Schreppler
10	343	Document Control
1	3421	TIC (C)
1	3422	TIC (A)